NASA-CR-201391

INSTITUTE FOR PHYSICAL RESEARCH AND TECHNOLOGY

IOWA STATE UNIVERSITY
AMES, IOWA 50011

SPACE LIFE-SUPPORT ENGINEERING PROGRAM

FINAL REPORT
NOVEMBER 1, 1993-APRIL 30, 1995

NASA GRANT NO. NAG 2-885

SUBMITTED TO DR. EDWIN L. FORCE
ADVANCED LIFE SUPPORT DIVISION
NASA-AMES RESEARCH CENTER 239-15
MOFFETT FIELD, CA 94035-1000

PRINCIPAL INVESTIGATOR
DR. RICHARD C. SEAGRAVE
DEPARTMENT OF CHEMICAL ENGINEERING
IOWA STATE UNIVERSITY
AMES, IOWA 50011

FINAL REPORT

Space Life Support Engineering Program
Iowa State University
Ames, Iowa

Period: November 1, 1993 through April 30, 1995

SUMMARY

This report covers the seventeen months of work performed under an extended one year NASA University Grant awarded to Iowa State University to perform research on topics relating to the development of closed-loop long-term life support systems with the initial principal focus on space water management. In the first phase of the program, investigators from chemistry and chemical engineering with demonstrated expertise in systems analysis, thermodynamics, analytical chemistry and instrumentation, performed research and development in two major related areas; the development of low-cost, accurate, and durable sensors for trace chemical and biological species, and the development of unsteady-state simulation packages for use in the development and optimization of control systems for life support systems. In the second year of the program, emphasis was redirected towards concentrating on the development of dynamic simulation techniques and software and on performing a thermodynamic systems analysis, centered on availability or exergy analysis, in an effort to begin optimizing the systems needed for water purification. The third year of the program, the subject of this report, was devoted to the analysis of the water balance for the interaction between humans and the life support system during space flight and exercise, to analysis of the cardiopulmonary systems of humans during space flight, and to analysis of entropy production during operation of the air recovery system during space flight.

PERSONNEL

Director: R. C. Seagrave, Distinguished Professor of Chemical Engineering

Graduate Research Assistant: Dasaratha Sridhar (entire period)
Major effort: Fault Detection Algorithm Development

Graduate Research Assistant: Sharmista Chatterjee (entire period)
Major effort: Thermodynamic Analysis, ASPEN Model Development of Integrated Physical-Chemical and Biological Systems

Graduate Research Assistant: Susan Doty (through December 1994)
Major effort: Physiological Water Model Development

Graduate Research Assistant:: Anca Stefanescu (entire period)
Major effort: Thermodynamic Analysis and Model Development

Graduate Research Assistant : Caroline Wilharm (entire period)
Major effort: Entropy production in the air recovery system

Graduate Research Assistant: Dawn Downey (entire period)
Major effort: Cardiovascular response for thermoregulation and oxygen consumption.

RESEARCH AND DEVELOPMENT PROGRESS

The research program is organized in three related, integrated, and highly-coupled projects designed to produce useable results over a five-year period. These projects address some of the unique problems of long-term closed-loop life support systems which are designed for periods of greater than 90 days. Among these are:

- Optimization of life-support systems to operate dynamically over a range of conditions which vary with the diet, exercise protocol, and environmental conditions of the crew

• Optimization of energy consumption and reduction of entropy generation by separation devices, processes, and systems.

• Optimization of process control strategies for conserving energy and material resources while maintaining environmental quality.

Progress during the period of the grant was made in the first two areas, and is summarized as follows.

1. Integration of a working model of the crew into a previously developed system model has been accomplished for the steady state. It is now possible to simulate the behavior of the system at steady state for different crew sizes, of differing physical characteristics and genders, and with different diets.

2. Progress on developing a dynamic model of the crew was accomplished in two areas. Susan Doty developed a dynamic model which will describe the unsteady state distribution of water in the body; that is the uptake, creation, sequestration, and outflow of water in humans as a function of diet, exercise protocol, and environmental factors. Initial development is being done using the dynamic simulation software package EXTEND. Details of this work are shown in Appendix 1. The second area of dynamic modeling is the further development of a model of thermoregulatory and fuel depletion aspects of humans- the description of the onset of hyperthermia, hypothermia, dehydration, or glycogen depletion as a function of exercise protocol and environmental parameters. This work, which was begun by Megan Scherb in 1992, has been extended by Dawn Downey who was also supported by the NASA grant. A summary of Downey's work to date is shown in Appendix 2..

3. The importance of availability analysis (exergy analysis) has continued to be a concern as the life support system becomes more complex and as biological interfaces become more numerous. Our preliminary results in this area are described in a paper by Chatterjee and Seagrave that was presented at the 1993 International Conference on Environmental Sciences in July 1993. A copy is attached as Appendix 3. Present efforts by Anca Stefanescu and Caroline Wilharm are directed towards the development of more rigorous energy and entropy balance equations or unsteady-state, open, complex systems with large numbers of chemical reactions occurring. A summary of their results is attached as Appendix 4.

APPENDIX 1

DYNAMIC SIMULATION OF WATER AND ELECROLYTE REDISTRIBUTION FOR HUMANS IN CLOSED-LOOP LIFE SUPPORT SYSTEMS

S. E. Doty, R. C. Seagrave
Iowa State University

ABSTRACT

When one is exposed to microgravity, fluid which is normally pooled in the lower extremeties is redistributed headward and weight bearing bones begin to demineralize due to reduced mechanical stresses. The kidney, which is the primary regulator of body fluid volume and composition, responds to the fluid shift and bone demineraliztion by increasing the urinary output of water, sodium, and calcium. This research involves developing a mathematical description of how water and electrolytes are internally redistributed and exchanged with the environment during space flight. This model consequently involves kidney function and the associated endocrine system. The model agrees well with actual data, including that a low sodium diet can prevent bone demineralization, therefore, assumptions made to develop the model are most likely valid. Since a life support system is responsible for controlling the environment, results from the model can aid in the design and development of such systems.

NOMENCLATURE

Symbol	Description	Typical Value
A	concentration of angiotensin II in plasma (ng/l)	27.0
ADH	concentration of ADH in plasma (munits/l)	4.0
ALD	concentration of aldosterone in the plasma (ng/l)	85.0
C	concentration of cortisol in the plasma (mg/l)	0.15
Ca^{++}	concentration of ionized calcium in plasma (mg/l)	55
CO	cardiac output (l/min)	5.0
D_{ADH}	clearance rate of ADH (l/min)	0.206
D_C	clearence rate of cortisol (l/day)	144
D_{PTH}	clearance rate of PTH (l/day)	3334
DV_E	excess fluid in extracellular compartment (l)	0.0
$D_{1,25(OH)2D3}$	clearence rate of 1,25-$(OH)_2D_3$ (l/day)	2.4
$FAb_{Ca^{++},int}$	fraction of ingested and secreted calcium which is absorbed by the intestine (dimensionless)	0.5
$F_{Na,DT}$	rate of flow of sodium into the distal tubule (mEq/min)	0.89
$F_{Na,LH}$	rate of flow of sodium into the loop of Henle (mEq/min)	4.44
$F_{Na,PT}$	filtered load of sodium (mEq/min)	17.75
$F_{Na,U}$	rate of excretion of sodium (mEq/min)	0.128
$FRe_{Ca^{++},DT}$	fraction of calcium delivered to the distal tubule which is reabsorbed by the distal tubule and collecting duct	0.61
$FRe_{W,LH}$	fraction of water reabsorbed in the loop of Henle	0.33
FT	flight time (day)	*
$F_{W,DT}$	rate of flow of water into the distal tubule (ml/min)	
$F_{W,LH}$	rate of flow of water into the loop of Henle (ml/min)	31.25

$F_{W,U}$	urine flow rate (ml/min)	1.0
GFR	glomerular filtration rate (ml/min)	125.0
GTB	fraction of filtered load of sodium reabsorbed in the proximal tubule	0.75
K_1	bone formation rate constant (l/day)	9.27
K_2	bone destruction rate constant (mg/day)	510
Na_i	intracellular concentration of sodium (mEq/l)	10.0
Na_{pl}	extracellular concentration of sodium (mEq/l)	142.0
1,25-$(OH)_2D_3$	concentration of 1,25-dihydroxycholecalciferol in plasma (mg/l)	0.00003
P_{ar}	arterial pressure (torr)	100.0
$P_{m,s}$	mean systemic pressure (torr)	7.0
PTH	concentration of parathyroid hormone in the plasma (mg/l)	0.00045
R	concentration of renin in plasma (GU/l)	0.06
$Re_{Na,DT}$	rate of reabsorption of sodium from the distal nephron segments (mEq/min)	0.757
$Re_{Na,LH}$	rate of reabsorption of sodium from the loop of Henle (mEq/min)	3.55
$Re_{Na,PT}$	rate of reabsorption of sodium from the proximal tubule (mEq/min)	13.3
$Re_{W,DT}$	rate of reabsorption of water in the distal nephron segments (ml/min)	19.7
$Re_{W,LH}$	rate of reabsorption of water in the loop of Henle (ml/min)	10.55
$Re_{W,PT}$	rate of water reabsorption in the proximal tubule (ml/min)	93.75
R_f	rate of calcium input to the bones (mg/day)	510
$R_{f,actual}$	rate of calcium input to the bones when the plasma cortisol level is elevated (mg/day)	*
R_r	rate of calcium output from the bones (mg/day)	510
$R_{r,actual}$	rate of calcium output from the bones when the plasma cortisol level is elevated (mg/day)	*
$R_{t,p}$	total peripheral resistance (torr/l· min)	20.0
S_A	rate of formation of angiotensin II (ng/min)	105.0
S_{ADH}	release rate of ADH (munits/min)	0.825
$S_{ADH,P}$	release rate of ADH due to plasma osmolality (munits/min)	0.84
$S_{ADH,V}$	release rate of ADH due to diminished fluid volume (munits/min)	0.81
S_{ALD}	rate of secretion of aldosterone (ng/min)	52.7
Sc	Schmidt number (dimensionless)	*
S_C	secretion rate of cortisol (mg/day)	21.6
$S_{Ca,B}$	net rate of ionized calcium release by the bones (mg/day)	0
$S_{Ca,I}$	net rate of ionized calcium absorbtion by the intestine (mg/day)	178
SL	stress level (dimensionless)	0.83
S_{PTH}	rate of secretion of parathyroid hormone (mg/day)	1.51
S_R	rate of release of renin (GU/min)	0.008
$S_{1,25(OH)2D3}$	rate if secretion of 1,25-$(OH)_2D_3$ (mg/day)	0.00072
$U_{Ca,K}$	urinary loss of ionized calcium (mg/day)	178
V_{bl}	blood volume (l)	5.0
V_E	extracellular fluid volume (l)	15.0
V_I	intracellular fluid volume (l)	25.0
V_{pl}	plasma volume (l)	3.0
V_W	total body water (l)	40.0
$V_{W,L}$	body water contained in the lower extremities (l)	12
$V_{W,U}$	body water contained in the upper body (l)	28

(* determined from experimental conditions)

INTRODUCTION

This research is concerned with the development of a quantitative and reliable mathematical description of how humans produce, internally redistribute, and exchange water with their environment as a function of diet and environmental conditions. Since many electrolytes, such as sodium and calcium, are dissolved in the bodily fluids, their redistribution within the body is coupled with the movement of water and can therefore be incorporated into the proposed model. Such a mathematical description will serve to aid in the design and development of long-term closed-loop life support systems for space flight. Additionally, the research which leads to such a model will elucidate any unclear factors which govern the redistribution of water and electrolytes within the body and between the body and the environment.

Some of the conditions experienced during space flight, such as microgravity, will be addressed. Microgravity has been found to drastically alter the human water balance and also cause demineralization of weight bearing bones.

BACKGROUND INFORMATION

Body Water

Total body water can be divided into two main compartments. Extracellular water, which accounts for about 25% of the body weight, includes all of the water outside of the cells. Intracellular water, which accounts for about 30% of the body weight, includes all of the water contained within the cells. The extracellular and intracellular body water compartments are shown in figure 1. The relationships between individual compartments has been studied separately and this diagram shows our interpretation of how the pieces of information fit together.

As figure 1 illustrates, water enters the body through the gastrointestinal tract where it is absorbed by the intestines and enters the plasma compartment. Plasma is the liquid part of blood and normally accounts for about 55% of the total blood volume with the remaining 45% being composed of red blood cells. The movement of fluid between the plasma compartment and the other body water compartments is controlled by pressure gradients. Water is lost from the body through four primary routes: sensible perspiration, insensible perspiration, urine, and feces. Water lost by sensible perspiration, or sweating, is a necessary part of the body's temperature control mechanism; water loss in feces accompanies the elimination of undigested food materials and other waste products; and water losses through diffusion and evaporation (insensible perspiration) are largely unavoidable [1]. Therefore, through the formation of urine, the kidneys provide the primary mechanism by which water loss is regulated.

The kidneys are the principal regulator of the body water compartments, and they carry out this function by altering the composition of the circulating plasma. As shown in figure 1, the kidneys filter fluid from the plasma compartment and components that the body wants to retain, such as glucose, vitamins, and electrolytes are reabsorbed and returned back to the plasma compartment. Components that the body does not want to retain, such as metabolic wastes, are not reabsorbed by the kidney and are subsequently excreted from the body in the form of urine.

Regulation of Kidney Function

The primary factors which regulate kidney function are arterial pressure, antidiuretic hormone (ADH), and aldosterone (ALD). Arterial pressure, which at rest is a function of the blood volume, controls the rate at which fluid is filtered from the plasma compartment and to the kidneys. A higher pressure produces a higher filtration rate. Consequently, arterial pressure determines the ensuing urine flow rate. Antidiuretic hormone, which is secreted from the pituitary gland, is released into the plasma when the plasma becomes too concentrated or when the plasma compartment is depleted. Antidiuretic hormone causes the kidneys to reabsorb more water and therefore tends to dilute the plasma while increasing the plasma volume. Since antidiuretic hormone controls the amount of water which is reabsorbed by the kidneys, it will determine the

urine concentration. The adrenal gland secretes aldosterone into the plasma in response to low sodium levels. Aldosterone causes the kidney to reabsorb more sodium and therefore will tend to increase the amount of sodium in the body. Consequently, aldosterone will affect the urine sodium concentration.

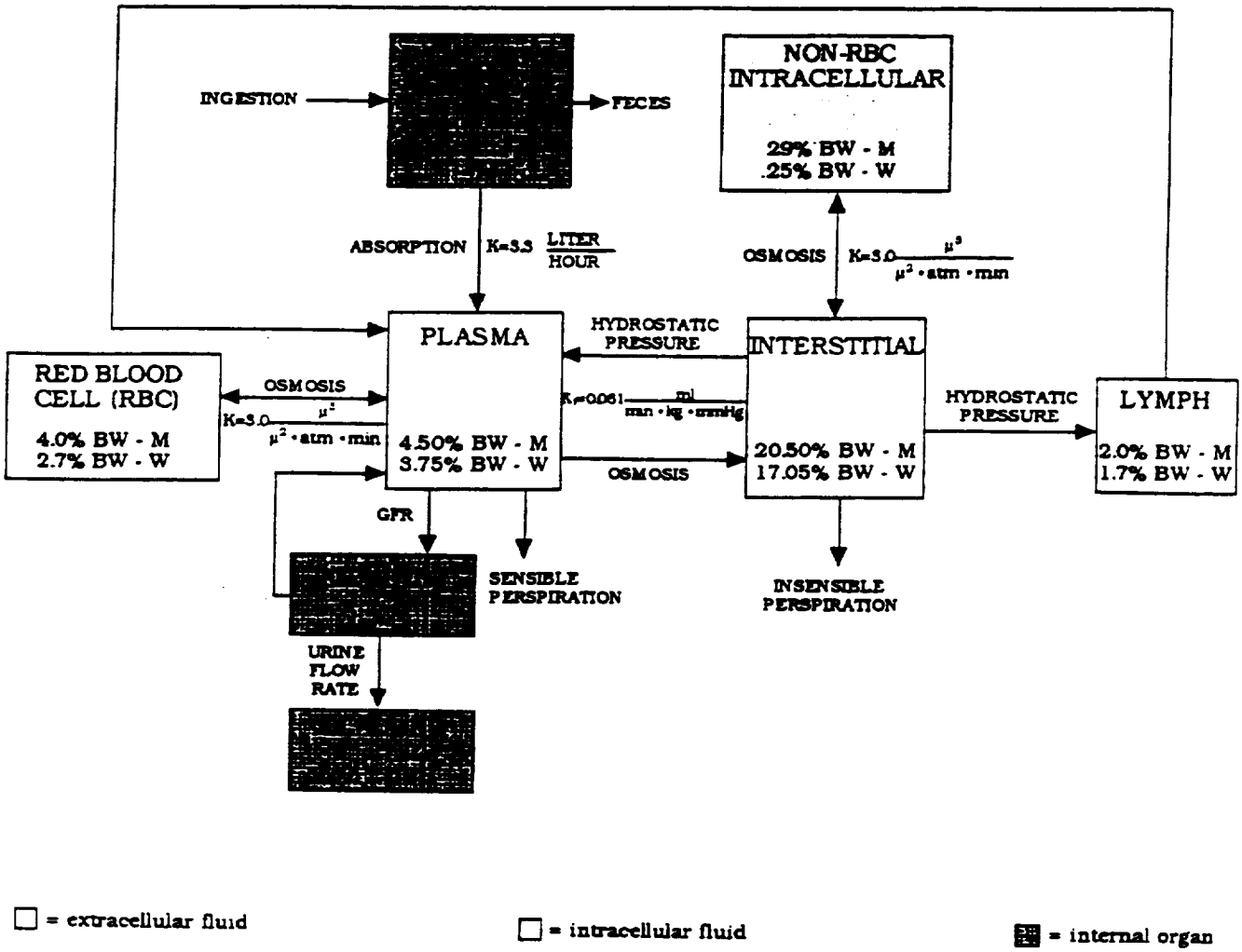

Figure 1: Body water compartments and the forces which cause flow between them. Membrane permeability is represented by K. The size of each compartment is shown for both males (M) and females (F) where BW = body weight.

MODELING KIDNEY FUNCTION

Description of the Kidney

The kidneys are shaped similar to lima beans and weigh about 300 grams apiece. The nephron is the functional unit of the kidney and consists of a renal tubule and an expanded end or Bowman's capsule (see figure 2). Each human kidney contains about 1.3 million nephrons. The Bowman's capsule surrounds a capillary bed, the glomerulus, which receives blood through an afferent arteriole and discharges blood, less some filtrate, through an efferent arteriole. The hydrostatic pressure within the glomerulus causes fluid to be filtered from the blood stream and into the Bowman's capsule. This fluid is very similar in composition to that of plasma. Typically, 180 liters of fluid enter the renal tubules each day although only about one liter of urine is produced due to the secretion and reabsorption processes which occur along the length of the nephron.

As seen in figure 2, the nephron can be divided into several, anatomically distinct, segments. The glomerular filtrate passes into the next nephron segment, the proximal tubule, due to a hydrostatic pressure gradient. This segment reabsorbs water and solutes in about the same proportion. As substances are reabsorbed, they are eventually returned back to the blood stream. By the time the tubular fluid reaches the next segment, the loop of Henle, 60 - 70% of the filtered solutes and water have been reabsorbed. The loop of Henle consists of a descending limb and an ascending limb, each of which have thin and thick segments. In general, the descending limb is freely permeable to water and relatively impermeable to solutes whereas the ascending limb is impermeable to water and the thick ascending limb actively reabsorbs sodium. The last portion of the nephron, the distal tubule and collecting tubule, are impermeable to water unless antidiuretic hormone is present in the extracellular fluid. The reabsorption of sodium from the tubular fluid within the distal tubule, and collecting tubule is controlled by the hormone aldosterone. Aldosterone stimulates ion pumps in these portions of the nephron, which then exchange sodium ions for potassium ions. Therefore, aldosterone increases the urinary loss of potassium while reducing this loss of sodium. From the collecting tubule, the filtrate passes through a ureter to the bladder.

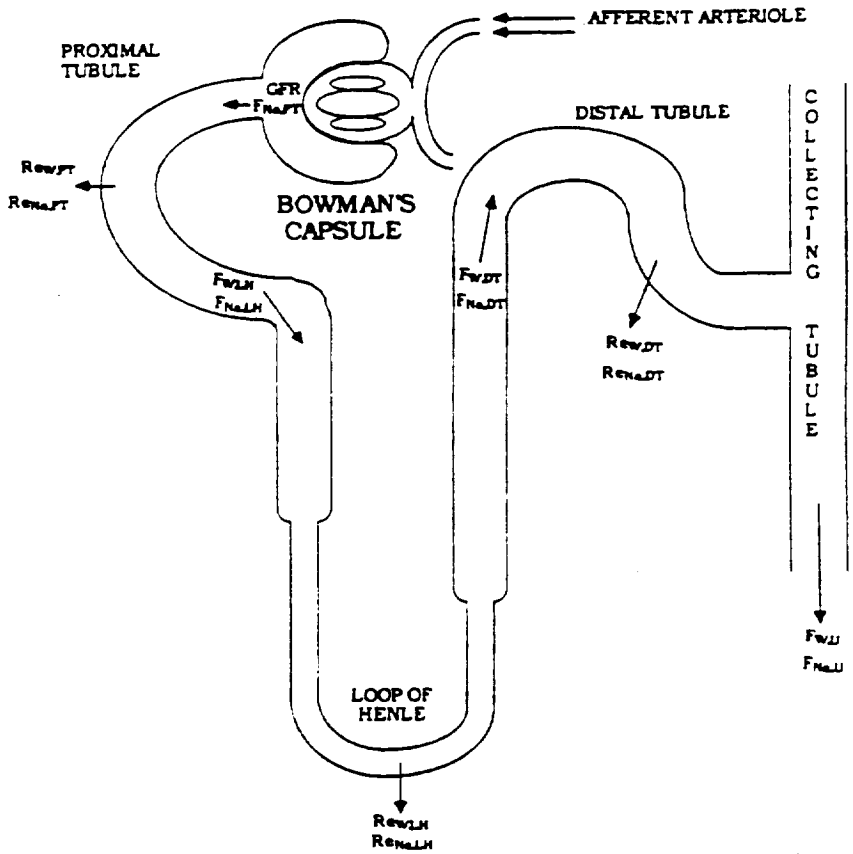

Figure 2: Nephron segments and the associated flow rates of water and sodium.

Sodium accounts for over 90% of the cations in the extracellular fluid [2]. Due to electroneutrality of the extracellular fluid, the amount of cations automatically controls the number of anions present, so by regulating the concentration of sodium, over 90% of the ions are also controlled. Consequently, sodium primarily determines the concentration of the extracellular fluid. In terms of regulating the body fluid compartments, the renal handling of water and sodium will be the most important factors to consider when modeling kidney function.

A mathematical model which describes kidney function in terms of arterial pressure, plasma antidiuretic hormone concentration, and plasma aldosterone concentration has been modified and adapted for out purposes [3]. Recall from the previous section that in terms of water and sodium

regulation, the primary factors which regulate kidney function are arterial pressure, antidiuretic hormone, and aldosterone. The model considers the reabsorption characteristics of each nephron segment and divides total body water into intracellular and extracellular compartments. For an averaged sized human, the total water volume is about 40 liters where the extracellular compartment accounts for 15 liters and the intracellular compartment accounts for the remaining 25 liters. The affect of arterial pressure, plasma antidiuretic hormone concentration, and plasma aldosterone concentration on the appropriate nephron segment is included. Plasma hormone and electrolyte concentrations are determined from mass balances whereas most other relationships have been derived from experimental data. These equations are given in appendix 1 and main features of the model are illustrated in figure 3.

Since sensible and insensible perspiration are lost from the extracellular compartment (see figure 1), these perspiration rates must be known. The insensible perspiration rate depends mainly on the skin temperature whereas the sensible perspiration rate depends mainly on the body core temperature and skin temperature. To determine the body temperatures a human thermoregulation model is used in conjunction with the kidney model. This model assumes a cylindrical body shape where the cylinder is divided into three layers which represent the body core layer, muscle layer, and skin layer. Energy balances are written for each layer and solved to determine the temperature of each layer.

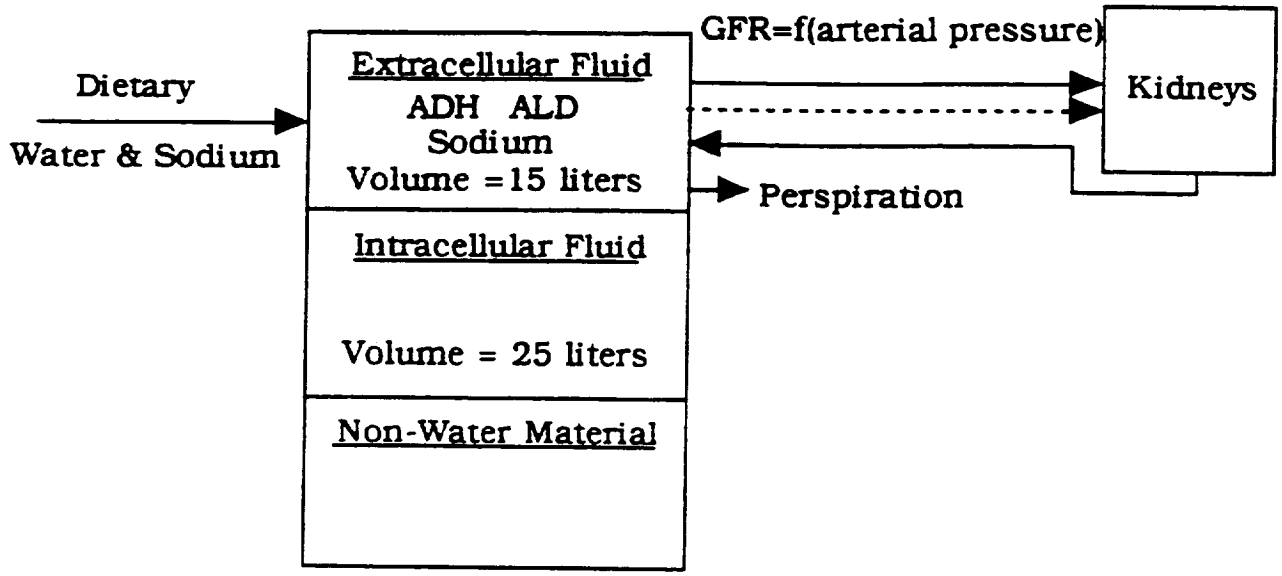

Figure 3: Illustration of the basic kidney model where plasma levels of ADH, ALD, and sodium are determined from mass balances whereas relationships between kidney function and arterial pressure, ADH, and ALD are determined experimentally. Solid line = flow of water and electrolytes. Dashed line = flow of other information.

Results predicted by the kidney model are compared with actual data in figure 4. For plot 4a, the urine flow rate increases because the plasma compartment is expanded and diluted. For plot 4b, the urine flow rate increases because sodium levels are elevated and the body must rid itself of the excess sodium.

SPACE FLIGHT

Water & Sodium Balance

On earth, the blood pressure in any vessel below the heart is increased and that in any vessel above the heart is reduced due to gravity. When one is exposed to microgravity, the hydrostatic pressure gradient in the body's blood column is diminished thereby decreasing the blood pressure

in the lower part of the body. Blood which is normally pooled in the lower extremities is then redistributed headward because the associated blood vessels are compressed by the elastic forces of the vessel walls. This fluid shift increases the central blood volume which increases the arterial pressure, decreases the antidiuretic hormone secretion rate, and consequently affects the kidney. The rate at which blood is transferred from the lower body to the upper body has been determined from ground-based experiments which eliminated the body's hydrostatic pressure gradient using a tilt table [6]. The experiments found that about 1 liter of fluid shifts from the legs over a two hour period and the functional relationship between the fluid shift rate and time is an exponential decay. The shift of water and sodium can be estimated by the following equations.

$$\text{Water volume shift (liters)} = 0.0135\exp(-0.015t) \qquad (1)$$

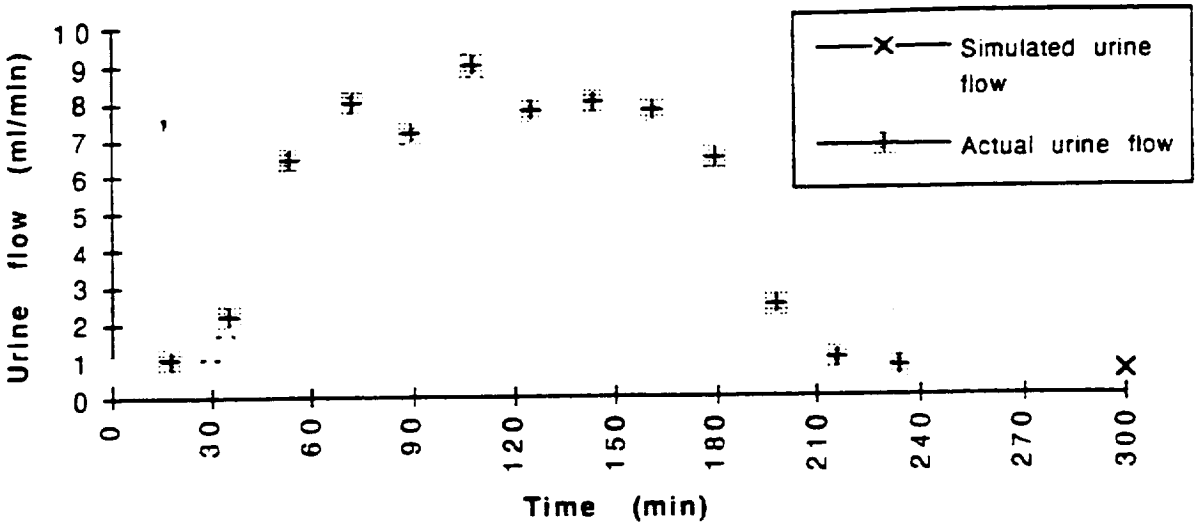

Figure 4a: Results from the model simulation and experimental data following ingestion of 1 liter of water. (actual data taken from [4])

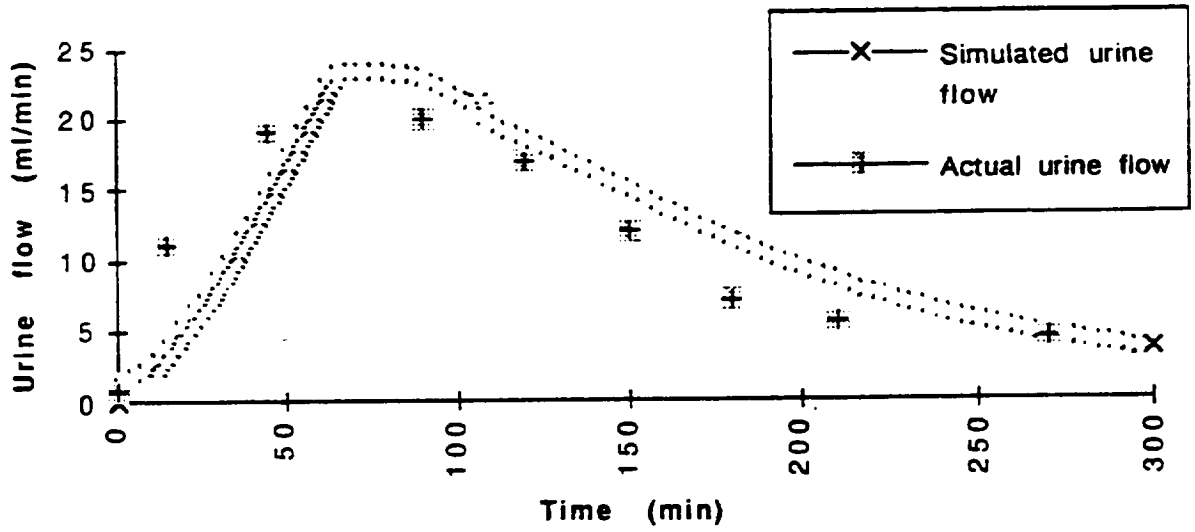

Figure 4b: Results from the model simulation and experimental data with infusion of 9.8 ml/min of a 10% NaCl solution during the first 65 minutes of the experiment. (actual data taken from [5])

Sodium shift (mEq) = 0.0608exp(-0.015t) (2)

To predict the urinary loss of sodium and water after exposure to weightlessness with the kidney model, the extracellular and intracellular body water compartments must be further divided into upper and lower body compartments. The kidneys are located near the center of the body and therefore respond to changes occuring in the upper body compartment. Fluid from the lower body compartment, or legs, is then transfer to the upper body compartment at the rates given by equations 1 and 2. For an averaged size person, total leg fluid volume is about 12 liters where approximately 4.5 liters are extracellular fluid and the remaining 7.5 liters are intracellular fluid. This model is illustrated in figure 5.

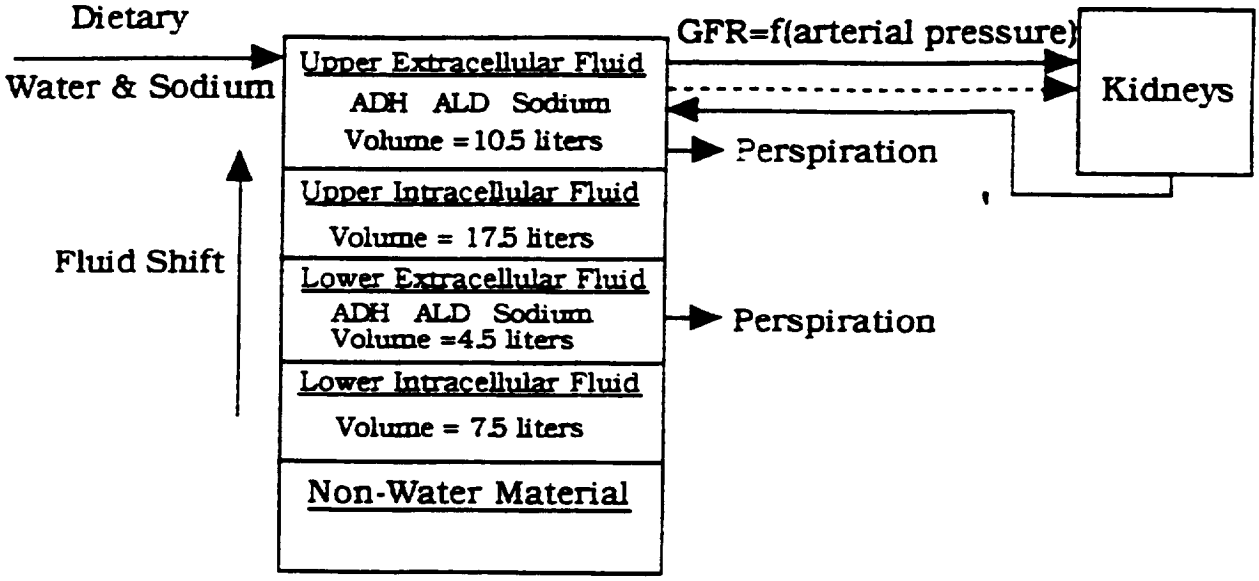

Figure 5: Illustration of the kidney model where the extracellular and intracellular fluid compartments have been divided to represent upper body water and lower body water for the simulation of weightlessness. Solid line = flow of water and electrolytes. Dashed line = flow of other information.

By dividing the extracellular and intracellular compartments as shown in figure 5 and including the fluid shift rates given by equations 1 and 2, the urine flow rate, arterial pressure, and antidiuretic hormone level can be predicted following the exposure to weightless conditions. Recall that arterial pressure is a function of upper body blood volume (see appendix 1) and blood volume also controls the antidiuretic hormone release rate (see Regulation of Kidney Function section). Predicted results are compared with actual data in figure 6.

Calcium Balance

Studies of astronauts have revealed abnormal losses of calcium and reduced bone density as a result of weightlessness incurred during space flight (Hattner, 1968). Although the precise mechanism of this calcium loss is not known, we have pieced together a proposed mechanism from available information. This mechanism is shown in figure 7.

It is believed that the reduced mechanical stresses on the skeleton experience during space flight causes the bone tissue to demineralize [7]. As the bone tissue demineralizes, calcium is released into the blood stream and consequently the plasma calcium concentration increases. The primary regulators of plasma calcium levels are parathyroid hormone and 1,25-dihydroxycholecalciferol. Parathyroid hormone, which is secreted by the parathyroid gland, is released into the plasma in

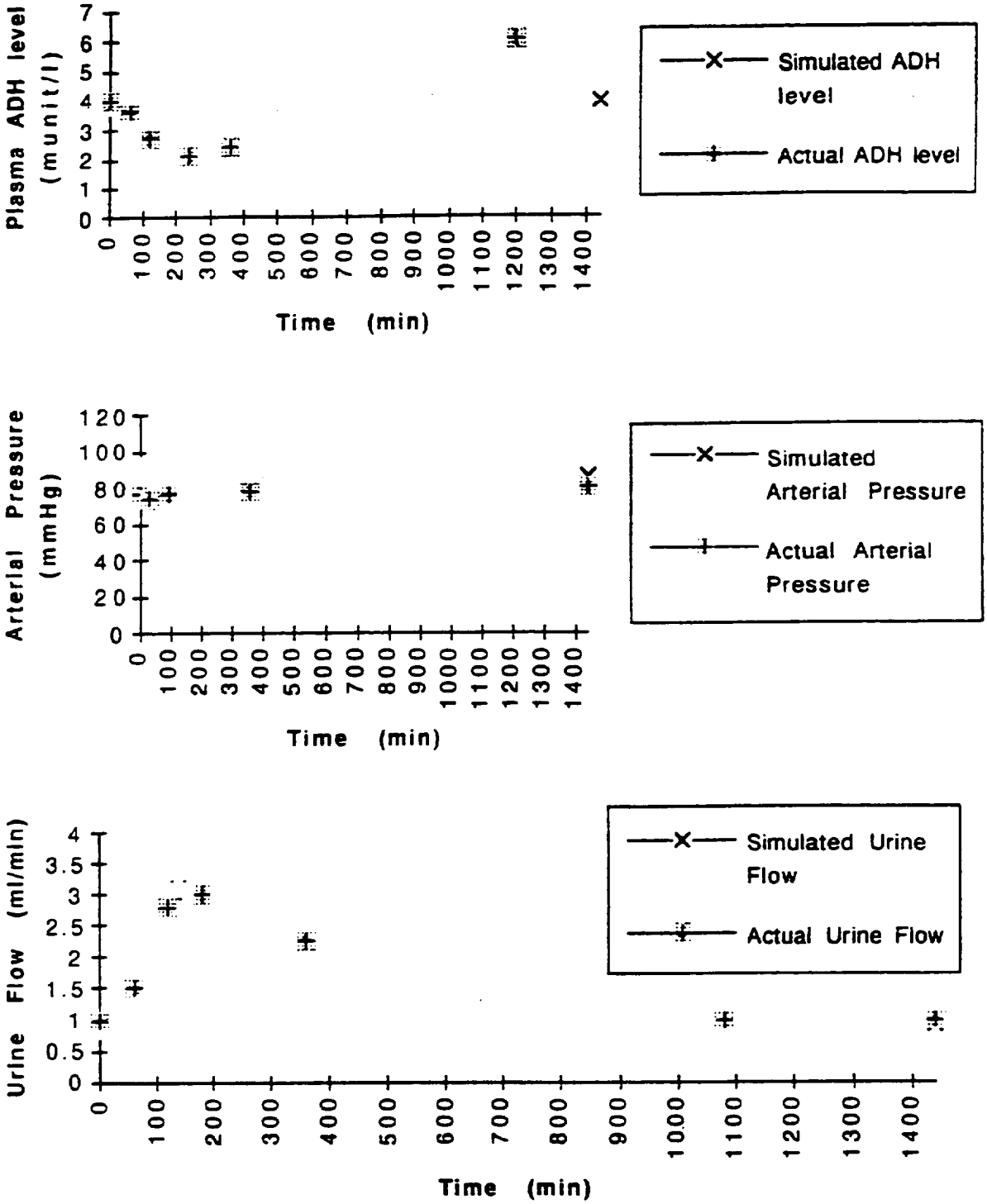

Figure 6: Comparison of results predicted by the model to actual data after exposure to weightless conditions. Plasma antidiuretic hormone concentration (top), arterial pressure (middle), and urine flow rate (bottom). (actual taken taken from [6]).

response to low plasma calcium levels. Parathyroid hormone increases plasma calcium levels by increasing the amount of calcium released from the bones (through bone reabsorption) and increasing the amount of calcium reabsorbed by the kidneys. Parathyroid hormone also stimulates the production of 1,25-dihydroxycholecalciferol. This hormone increases the intestinal absorption of calcium. Therefore, when the bones demineralize, plasma calcium levels increase thereby decreasing the secretion rate of parathyroid hormone and the subsequent production of 1,25-dihydroxycholecalciferol.

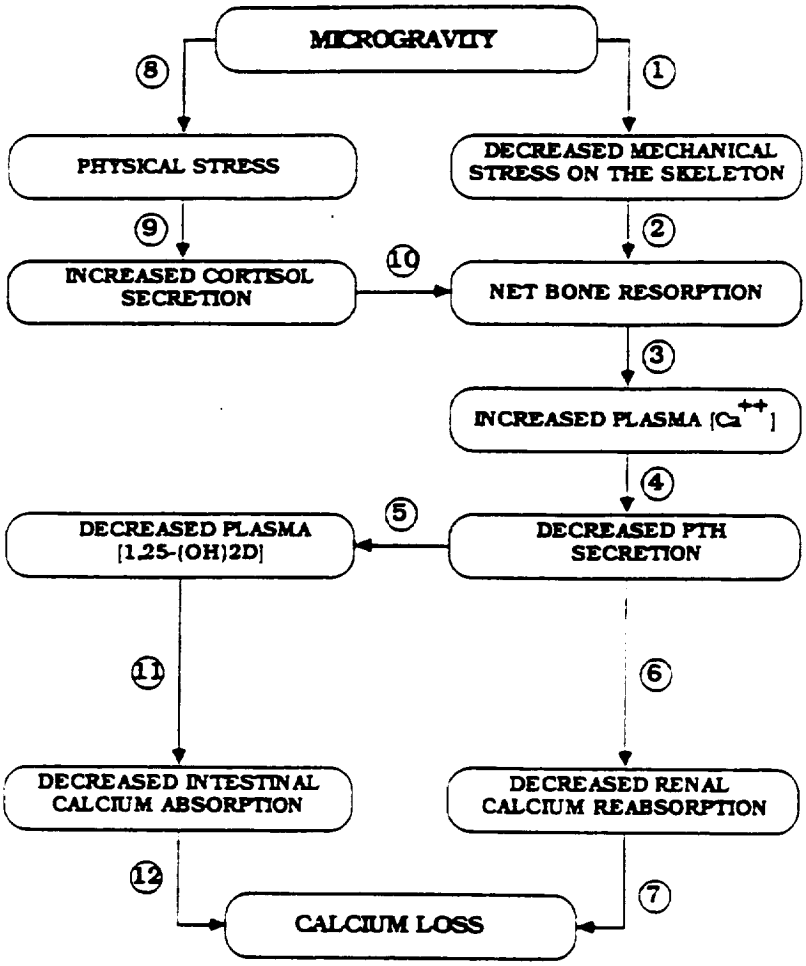

Figure 7: Proposed mechanism of calcium loss from the body during weightlessness.

Mathematical equations have been derived from experimental data and mass balances to describe the 12 relationships shown in figure 7. These equations are given in appendix 2. By incorporating these mathematical expressions with the kidney model diagrammed in figure 5, the human calcium balance during weightlessness can be estimated. When the ingested amount of calcium is known, the plasma calcium concentration, the urinary calcium loss, and the fecal calcium loss can be calculated with the model. The simulated values are compared with actual data in figure 8.

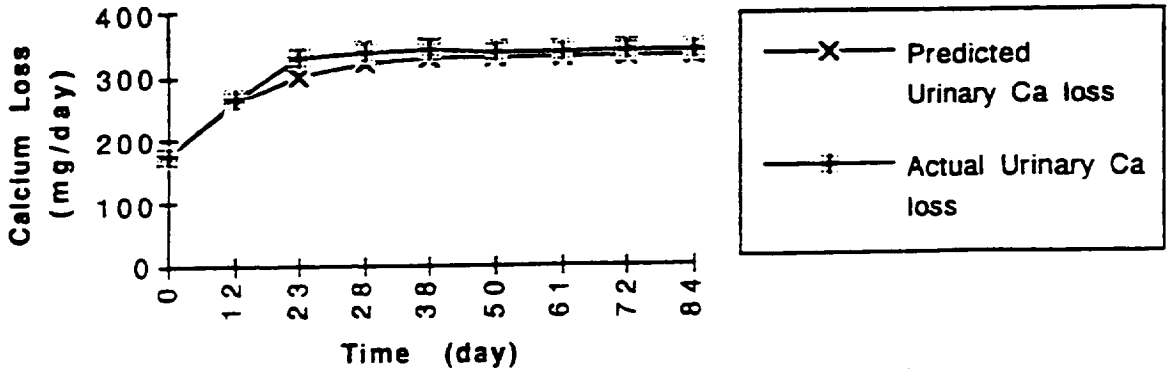

Figure 8a: Urinary calcium excretion during space flight. (actual data taken from [8])

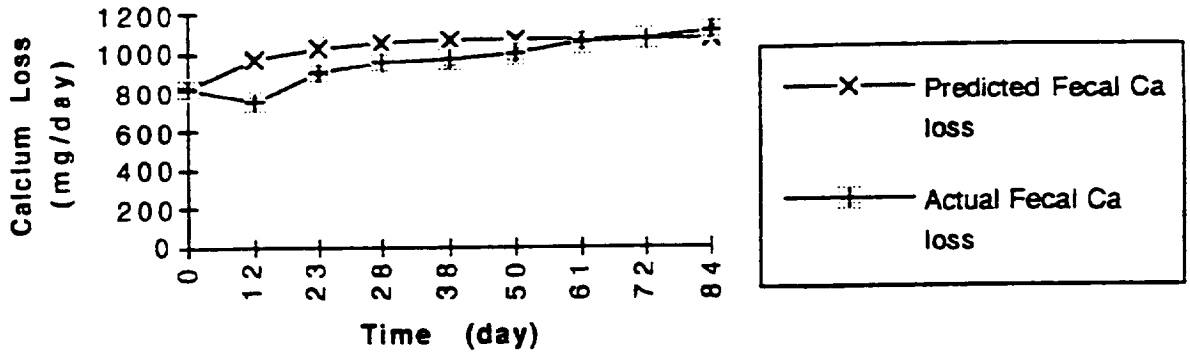

Figure 8b: Fecal calcium excretion during space flight. (actual data taken from [8])

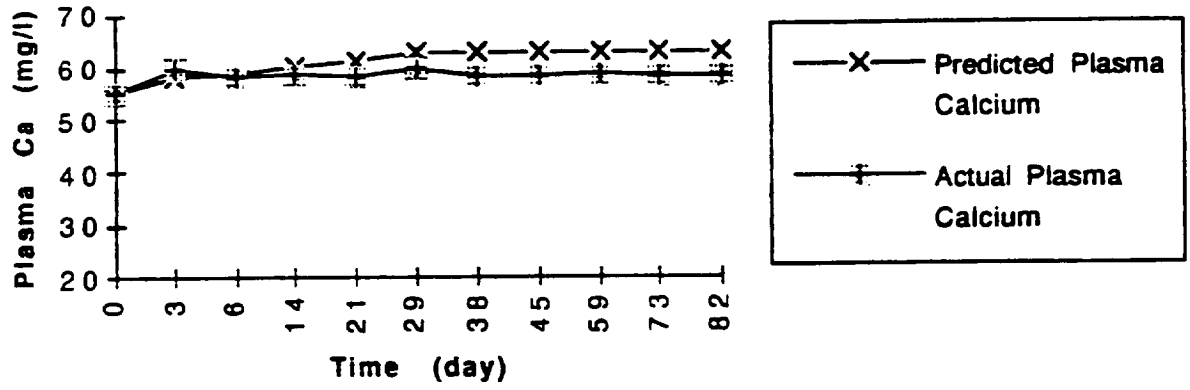

Figure 8c: Plasma calcium levels during space flight. (actual data taken from[8])

A previous study found that the increased urinary calcium loss which occurs during weightlessness could be eliminated if a low sodium diet was employed [9]. The study used a tilt-table to simulate weightlessness and the sodium intake was restricted to 110 meq/day. A normal sodium intake is about 170 meq/day. When sodium intake is restricted, the plasma sodium concentration decreases which stimulates the release of aldosterone. Aldosterone increases the amount of sodium reabsorbed by the nephron. Since calcium reabsorption is coupled to sodium reabsorption for the proximal tubule and loop of Henle (ie: identical fractions of sodium and calcium have been reabsorbed by the time the filtrate reaches the distal tubule) increasing sodium

reabsorption consequently increases calcium reabsorption. This action, which is considered in step 6 of figure 7, maintains a higher plasma calcium level and thereby stimulates the formation of new bone material. The urinary loss of calcium for the study is compared with the model prediction in figure 9.

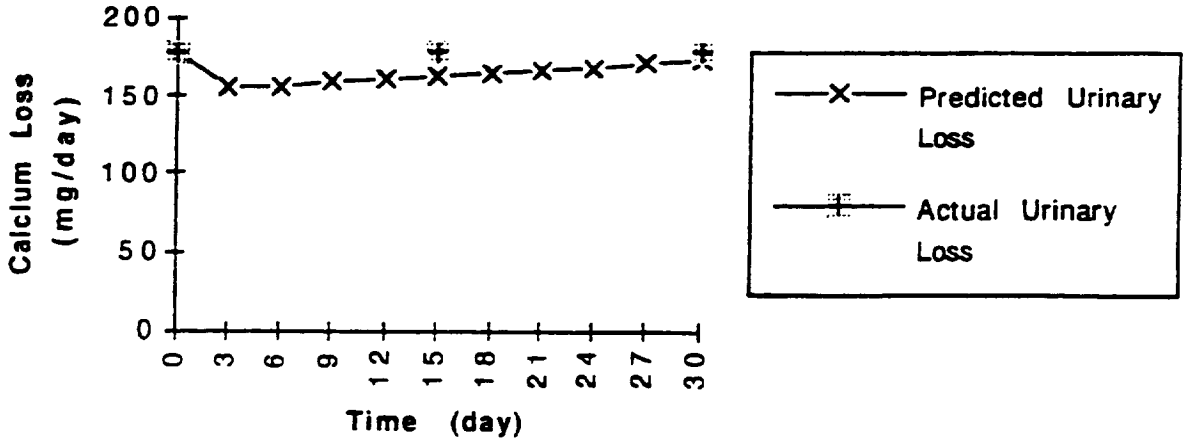

Figure 9: Urinary calcium excretion during head-down tilt where the sodium intake was restricted to 110 meq/day. (actual data taken from [9])

CONCLUSION

The water, sodium, and calcium balance on earth or during weightless conditions can be predicted by modeling kidney function and the associated endocrine system. The relationships used in the kidney model are determined either from experimental data or from mass balances. Water loss through perspiration, which is derived from the extracellular compartment, is a function of body temperature. A thermoregulation model can be used to estimate body temperature. With the kidney model and thermoregulation model, the output of water, sodium, and calcium from the body can be predicted for a variety of diets and environmental conditions. The balance of these substances is then determined by subtracting the output flows from the input flows.

This model has incorporated nephron reabsorption characteristics, arterial pressure, antidiuretic hormone level, aldosterone level, and parathyroid hormone level into the mathematical equations used to describe kidney function (see appendices 1 and 2). Consequently, mechanisms by which the human body regulates water, sodium, and calcium are included in the model. Methods of reducing the harmful effects of space flight on the human water, sodium, and calcium balance can therefore be explained by the model. For instance, a low sodium diet can prevent bone loss during weightlessness.

The success of long-term space flight critically depends upon the design characteristics of the life support system, since this system is responsible for providing an environment which can comfortable sustain human life. The design of such systems must include aspects of the crew's physiology and of the mechanical equipment which maintains the environment. This research provides some of the required physiological information.

ACKNOWLEDGMENTS

The authors would like to sincerely thank the organizations which supported this research, the Iowa Space Consortium and Nasa Ames (grant number NAG 2-885).

REFERENCES

1. Hole, J. W., ed. (1987), Human Anatomy and Physiology, 4th ed., Wm. C. Brown Publishers, Dubuque, Iowa. 966 pp.
2. Guyton, A. C., ed. (1984), Physiology of the Human Body, Saunders College Publishing, Philadelphia. 691 pp.
3. Uttamsingh, R. J., Leaning, M. S., Bushman,J. A., Carson, E. R., and Finkelstein, L. (1985), "Mathematical Model of the Human Renal System," Med. Biol. Eng. Comput., Vol. 23, pp. 525-535.
4. Baldes, E. J., and Smirks, F. H. (1934), "The Effect of Water Drinking, Mineral Starvation, and Salt Administration on the Total Osmotic Pressure of the Blood in Man, Chiefly in Relation to the Problems of Water Absorption and Water Diuresis," J. Physiol., Vol. 82, pp. 62-74.
5. Dean, R. F. A., and McCance, R. A. (1949), "The Renal Responses of Infants and Adults to the Administration of Hypertonic Solutions of Sodium Chloride and Urea," J. Physiol., Vol. 109, pp. 89-97.
6. Blomquist, C., Nixon,J. V., Johnson,R. L., and Mitchell, J. H. (1980), "Early Cardiovascular Adaptation to Zero Gravity Simulated by Head-Down Tilt," Acta Astronaut. Vol. 7, pp. 543-553.
7. Schneider, V. S., LeBlanc, A., and Rambaut, R. C. (1989), "Bone and mineral metabolism," Space Physiology and Medicine,1st ed., Lea & Febiger, Philadelphia, pp.214-221.
8. Rambaut, P. C., and Johnston, R.S. (1979). "Prolonged Weightlessness and Calcium Loss in Man," Acta Astronautica, Vol. 6, pp. 1113-1122.
9. Arnaud, S. B., Navidi, M., and Harper, J. (1993), "Urinary Calcium Loss and Dietary Sodium," Research and Technology 1993. Ames Research Center, Moffett Field, California.

APPENDIX 1

Experimentally Determined Equations Used in the Kidney Model

Mean systemic pressure ($P_{m,s}$) as a function of blood volume (V_{bl})

$$P_{m,s} = 3.5(V_{bl} - 3)$$

Cardiac output (CO) as a function of $P_{m,s}$

$$CO = 1.4(P_{m,s})$$

Total peripheral resistance ($R_{t,p}$) as a function of plasma angiotensin (A) level

$$R_{t,p} = 19 + 0.037[A] \quad \text{for } [A] \leq 27 \text{ ng/l}$$
$$R_{t,p} = 12.2 + 5.44\log[A] \quad \text{for } [A] > 27 \text{ ng/l}$$

Arterial pressure (P_{ar}) as a function of CO and $R_{t,p}$

$$P_{ar} = CO(R_{t,p})$$

This equation comes from the following relationship between flow and resistance in a hydraulic circuit

$$\text{Flow} = \frac{\Delta P}{\text{Resistance}}$$

Glomerular filtration rate (GFR) as a function of arterial pressure (P_{ar})

$$GFR = 4.50 - 1.62P_{ar} + 0.100(P_{ar})^2 - 1.2\times10^{-3}(P_{ar})^3 + 5.73\times10^{-6}(P_{ar})^4 - 9.89\times10^{-9}(P_{ar})^5$$

Chemical analysis of glomerular filtrate has found that it has approximately the same sodium concentration as plasma so the rate of filtration of sodium into the proximal tubule ($F_{Na,PT}$) is given by

$$F_{Na,PT} = GFR[Na_{pl}]$$

Reabsorption rate of sodium in the proximal tubule ($Re_{Na,PT}$)

$$Re_{Na,PT} = GTB(F_{Na,PT})$$
$$GTB = 5.815 - 0.0357[Na_{pl}]$$

Reabsorption rate of water in the proximal tubule ($Re_{W,PT}$)

$$Re_{W,PT} = GTB(GFR)$$

Reabsorption rate of sodium in the loop of Henle ($Re_{Na,LH}$)

$$Re_{Na,LH} = 0.8F_{Na,LH}$$

Reabsorption rate of water in the loop of Henle ($Re_{W,LH}$)

$$FRe_{W,LH} = -0.01F_{W,LH} + 0.65$$
$$Re_{W,LH} = FRe_{W,LH}(F_{W,LH})$$

In the distal and collecting tubules, the amount of water reabsorbed is controlled by antidiuretic hormone (ADH) and the amount of sodium reabsorbed by aldosterone (ALD).

Reabsorption rate of sodium in the distal and collecting tubules ($Re_{Na,DT}$)

$$Re_{Na,DT} = F_{Na,DT}(0.003[ALD] + 0.596) \quad \text{for } 0 \le [ALD] \le 85$$
$$Re_{Na,DT} = F_{Na,DT}(0.00021[ALD] + 0.833) \quad \text{for } 85 < [ALD] \le 800$$
$$Re_{Na,DT} = F_{Na,DT} \quad \text{for } [ALD] > 800$$

Reabsorption rate of water in the distal and collecting tubules ($Re_{W,DT}$)

$$Re_{W,DT} = 0.0 \quad \text{for } [ADH] \le 0.765$$
$$Re_{W,DT} = F_{W,DT}(0.383ADH - 0.293) \quad \text{for } 0.765 < [ADH] \le 3.0$$
$$Re_{W,DT} = F_{W,DT}(-0.0383[ADH]^2 + 0.364[ADH] + 0.109) \quad \text{for } 3.0 < [ADH] \le 5.0$$
$$Re_{W,DT} = F_{W,DT}(0.0012[ADH] + 0.9653) \quad \text{for } 5.0 < [ADH]$$

Secretion rate of antidiuretic hormone (S_{ADH}) as a function of the amount of excess fluid in the extracellular compartment (DV_E) and the plasma osmolality which is related to the plasma sodium concentration [Na_{pl}].

$$S_{ADH,P} = 0.2374[Na_{pl}] - 32.89 \quad \text{for } [Na_{pl}] \ge 138.5 \text{ mosm/l}$$
$$S_{ADH,P} = 0.0 \quad \text{for } [Na_{pl}] < 138.5 \text{ mosm/l}$$
$$S_{ADH,V} = 0.0 \quad \text{for } DV_E \ge 1.8$$
$$S_{ADH,V} = 0.15 - 0.083DV_E \quad \text{for } 1.8 > DV_E \ge 1.0$$
$$S_{ADH,V} = 0.813 - 0.75DV_E \quad \text{for } 1.0 > DV_E \ge -1.2$$
$$S_{ADH,V} = 1.71 \quad \text{for } -1.2 > DV_E$$
$$S_{ADH} = \frac{S_{ADH,V} + S_{ADH,P}}{2.0}$$

Rate of clearance of ADH from the plasma compartment (D_{ADH})

$$D_{ADH} = 0.206 \quad \text{for } [ADH] > 4.0 \text{ munits/l}$$
$$D_{ADH} = 0.374 - 0.042\,[ADH] \quad \text{for } [ADH] \le 4.0 \text{ munits/l}$$

Renin controls the rate at which angiotensin II is formed and angiotensin II controls the aldosterone secretion rate.

Secretion rate of renin (S_R) into the plasma compartment

$S_R = 0.0163 - 0.0093F_{Na,DT}$

Rate of clearance of renin (D_R) from the plasma compartment

$D_R = 0.143$ l/min

Secretion rate of angiotensin II (S_A) into the plasma compartment

$S_A = 583[R](V_{pl})$

Rate of clearance of angiotensin II (D_A) from the plasma compartment

$D_A = 3.78$ l/min

Secretion rate of aldosterone (S_{ALD}) into the plasma compartment

$S_{ALD} = 0.75[A] + 7.76$ for [A] < 18 ng/l

$S_{ALD} = 3.32[A] - 38.5$ for $18 \leq [A] < 34.0$

$S_{ALD} = 0.585[A] + 54.6$ for $[A] \geq 34.0$

Rate of clearance of aldosterone (D_{ALD}) from the plasma compartment

$D_{ALD} = 0.602$ l/min

Mass Balance Equations Used in the Kidney Model

Flow rates of sodium and water into the loop of Henle, distal and collecting tubules, and the urine flow rate.

$F_{Na,LH} = F_{Na,PT} - Re_{Na,PT}$

$F_{W,LH} = F_{W,PT} - Re_{W,PT}$

$F_{Na,DT} = F_{Na,LH} - Re_{Na,LH}$

$F_{W,DT} = F_{W,LH} - Re_{W,LH}$

$F_{Na,U} = F_{Na,DT} - Re_{Na,DT}$

$F_{W,U} = F_{W,DT} - Re_{W,DT}$

The plasma hormone levels and sodium level can be determined from a mass balance on the plasma compartment where accumulation = input - output. For the hormonal substances (SUB)

$$(V_{pl})\frac{d[SUB]}{dt} = S_{SUB} - D_{SUB}[SUB]$$

where S represents the input or secretion rate and D represents the clearance rate.

APPENDIX 2

Equations Used in the Calcium Balance

For the steps illustrated in figure 7.

Step 2 - Reduced mechanical stress causes the body to accelerate bone reabsorption (R_r) and slow down or maintain bone formation (R_f).

$R_r = K_2$

$R_f = K_1[Ca^{++}]$

where

$K_1 = 9.27$ l/day for conditions of earth

$K_2 = 510$ mg/day for conditions of earth

$K_1 = 13.5$ l/day for bed rest conditions

$K_2 = 815$ mg/day for bed rest conditions

Step 3 - calcium concentration $[Ca^{++}]$ in the extracellular compartment

$$V_E \frac{d[Ca^{++}]}{dt} = S_{Ca,B} + S_{Ca,I} - U_{Ca,K}$$

Step 4 - plasma calcium concentration [Ca++] affects the secretion rate of parathyroid hormone (S_{PTH})

$$S_{PTH} = -0.0749[Ca^{++}] + 5.62$$

The rate of clearance of parathyroid hormone (D_{PTH}) from the plasma compartment

$$D_{PTH} = 3334 \text{ liter/day}$$

From a mass balance of parathyroid hormone in the plasma compartment

$$(V_{pl})\frac{d[PTH]}{dt} = S_{PTH} - D_{PTH}[PTH]$$

Step 5 - The plasma parathyroid hormone concentration [PTH] affects the secretion rate of 1,25-$(OH)_2D_3$ ($S_{1,25(OH)_2D_3}$).

$$S_{1,25(OH)_2D_3} = 1.6[PTH]$$

The rate of clearance of 1,25-$(OH)_2D_3$ ($D_{1,25-(OH)_2D_3}$) from the plasma compartment.

$$D_{1,25-(OH)_2D_3} = 2.4 \frac{\text{liter}}{\text{day}}$$

From a mass balance on 1,25-$(OH)_2D_3$ in the plasma compartment.

$$(V_{pl})\frac{d[1,25-(OH)_2D_3]}{dt} = S_{1,25-(OH)_2D_3} - D_{1,25-(OH)_2D_3}[1,25-(OH)_2D_3]$$

Step 6 - parathyroid hormone affects renal calcium reabsorption. For nephron segments up to the renal tubule, the fraction of calcium reabsorbed is approximately the same as the fraction of sodium reabsorbed. The fraction of calcium reabsorbed ($FRe_{Ca^{++},DT}$)in the distal and collecting tubules,

$$FRe_{Ca^{++},DT} = 1366[PTH]$$

Step 7 - The urinary calcium loss ($U_{Ca,K}$) decreases the amount of calcium in the body (see step 3)

Step 9 - The physical and emotional stress experienced during space flight affects the secretion rate of cortisol (S_C).

$$S_C = 25.9(SL)$$

$$SL = 0.0197(FT) + 0.83 \quad \text{for } FT \leq 30 \text{ days}$$

$$SL = 1.42 \quad \text{for } FT > 30 \text{ days}$$

The rate of clearance of cortisol (D_C) from the plasma compartment.

$$D_C = 144 \text{ l/day}$$

From a mass balance on cortisol in the plasma compartment.

$$V_E\frac{d[C]}{dt} = S_C - D_C[C]$$

Step 10 - cortisol stimulates bone resorption (R_r) and inhibits bone formation (R_f).

$$R_{f,actual} = K_1[Ca^{++}]\{-0.00126[C] + 1.189\}$$

$$R_{r,actual} = K_2\{0.0002[C] + 0.9703\}$$

where $R_{f,actual}$ and $R_{r,actual}$ and the rates when the cortisol level is elevated.

Step 11 - 1,25-$(OH)_2D_3$ affects the fraction of ingested calcium absorbed by the intestine ($FAb_{Ca^{++},int}$).

$$FAb_{Ca^{++},int} = 10{,}000[1,25-(OH)_2D_3] + 0.20$$

Step 12 - the net intestinal calcium absorption ($S_{Ca,I}$) is decreased when $FAb_{Ca^{++},int}$ is decreased. This action decreases the total amount of calcium is the body (see step 3).

APPENDIX 2

A COUPLED MODEL OF THE CARDIORESPIRATORY AND THERMOREGULATORY SYSTEMS: OXYGEN TRANSPORT VS. THERMOREGULATION

Dawn Downey and R. C. Seagrave
Department of Chemical Engineering
Iowa State University, Ames, Iowa 50011

Numerous mathematical models of the circulatory system have been developed to describe blood flows that carry oxygen, carbon dioxide, and water, but most of them have not included the changes in temperature which are also occurring. The coupled model in this work combines these approaches in order to better predict the thermoregulatory and circulatory effects resulting from dynamic changes from steady-state behavior. When a person exercises, for example, increased muscle blood flow is required to deliver additional oxygen to muscles. Blood flow to the skin usually also needs to be increased to meet the growing demand for heat transfer resulting from more heat being produced by the muscles. At least 80 percent of the energy released by oxygen consumption must go to thermal forms and ultimately, be dissipated as heat from the skin and respiratory tract. (Mitchell, 1977)

Quite separately, models have been developed to describe thermoregulation in the human body. Many of them are based on the "three cylinder" approach which divides the body into three distinct layers consisting of core, muscle, and skin which are "wrapped around" each other. While this simple approach is fairly good for modeling conductive transport, that is, temperature changes produced by heat conducted between adjacent materials of different temperatures, it often ignores or approximates the heat being exchanged through convective means. Since blood is flowing between and among the different layers, heat exchange is also being performed by the vascular system.

In this work, we believe that the next important step in the development of this type of model should be to combine it with a metabolic-based circulatory modeling approach which includes a rational description of all the significant control factors and phenomena present. Leigh described some early attempts to do this in which the body was divided into tissue and lung compartments, with metabolism being added to the tissues and heat being exchanged with the environment. (Leigh, 1984) Temperature was considered to be uniform throughout the body, however, and only one energy balance was included. This is clearly an inadequate description of human thermoregulation. Since blood flow carries heat, oxygen, and carbon dioxide, a combined approach is necessary to understand the changes and limitations that take place when an external effect, such as exercise level, ambient temperature, or gravity is altered.

First we must ask the question, how are increases in blood flow accomplished? Some possible mechanisms include; a re-direction of the blood flow from certain internal organs to the periphery of the body (muscles and skin), an increased cardiac output due to an increased heart rate or more fluid being taken up by the blood stream, or a combination of these mechanisms.

Partitioning of increased blood flow to skin from working muscles during exercise will limit the delivery of oxygen to muscles and, thus, reduce the ability to maintain a high rate of ATP resynthesis, which represents the energy production required in exercising. Partitioning more blood flow to muscles from skin, however, will limit the rate of heat transfer from the core to the skin, causing a rapid rise in the body core temperature. Theories of Rowell, et al. suggest that instead of either of these mechanisms, blood flow through specialized tissue beds is reduced during exercise, e.g., splanchnic and renal blood flow have been shown to decrease during increased levels of exercise. (Nadel, 1980) They suggest that this might compensate for the increased need of the skin, which requires extra blood flow to transfer some of the additional heat produced during mild or moderate exercise to the surroundings. In fact, Rowell (1974) determined that vasoconstriction of these two regions during moderate exercise under heat stress could account for the redistribution of 600 to 800 ml/min of blood flow to the skin. At maximum vasoconstriction of splanchnic and renal blood vessels, about 2.2 L/min of blood flow can be redistributed to working muscles and/or skin. Both the metabolic and temperature regulation requirements are probably not capable of being met at higher levels of exercise or exercise performed under heat stress through blood flow partitioning, however, and cardiac output must be increased.

Increased blood flow to the periphery will reduce central (core) blood volume, reducing cardiac filling pressure and compromising stroke volume. When stroke volume is reduced with the heart rate being held constant, cardiac output is also reduced because a smaller volume of blood is expelled from the heart in the same amount of time. If heart rate is correspondingly increased, cardiac output can be maintained and will even increase in proportion to oxygen uptake, but this compensatory response has limits. During low to moderate exercise in cool conditions, cardiac output typically does not change much, but A-V oxygen difference (the difference between the oxygen concentration in the arteries and the veins) increases (with increasing oxygen uptake) and heart rate increases to compensate for the decreased stroke volume. (Ekelund, 1967) A maximum cardiac output of around 22 L/min (approximately a four fold increase from rest) can be reached in a typical person with a maximum oxygen uptake of 3.7 L/min in a relatively cool environment. (Rowell, 1977)

If the exercise is continued to very high levels, vasoconstriction occurs whereby blood vessels become smaller to keep blood in the core and maintain stroke volume. When this happens, the rate of heat transfer from the core to the skin becomes insufficient and core temperature continues to rise. It has been shown in numerous experiments that metabolic circulatory regulation will be given precedence over temperature regulation in this case. (Nadel, 1980)

Cutaneous vasoconstriction is just one reflex which will favor oxygen delivery at the expense of thermoregulation. Increases in cutaneous venomotor tone and an increasing degree of tone during exercise will occur. (Nadel, 1980) Thirdly, an upward shift in the core temperature threshold for cutaneous vasodilation will cause blood to shift toward the core by making the blood vessels of the skin stay constricted, even at higher temperatures. (Nadel, Fortney, and Wenger, 1980) All of these reflexes will help to maintain the core blood volume (stroke volume), but will also reduce the heat transfer rate from the core to the skin. (Nadel, 1983)

Early theories often supported the idea that, during maximal exercise, only the metabolic demands of the exercising muscles are important. As a result of these measures which serve to protect the metabolic circulatory demands, many cardiovascular researchers tended to ignore thermoregulatory effects. But more recent evidence shows that heat dissipation is also an important consideration. The central circulation can often meet increased demands for heat dissipation so "...thermoregulatory factors can influence the central circulation during exercise". (Saltin, 1970)

Circulatory requirements of the muscles are favored over those of the skin when a competition exists, but they must also be limited. Exercise cannot be increased indefinitely, and oxygen uptake reaches a maximum at some point beyond which the subject cannot continue to use a higher rate of oxygen by the muscles. This has been shown to occur, typically, when about 80 to 85 percent of the cardiac output perfuses active muscles while inactive tissues are maximally vasoconstricted. (Rowell, 1974) The maximum oxygen uptake of a certain individual is set by many factors such as their degree of training. Many have hypothesized that circulatory delivery of oxygen is the single limiting step in the maximum oxygen uptake that is attainable. It has been shown that the rate of increase in cardiac output declines as the oxygen uptake approaches its maximum. (Saltin, 1964)

Ambient temperature is another important factor in determining the behavior of the body's circulation. Brouha was one of the first to propose (in 1960) that cardiac output should increase during exercise in the heat to meet increased circulatory requirements and prolong the amount of work possible. (Nadel, Cafarelli, Roberts, and Wenger, 1979) At rest, cardiac output remains relatively unchanged up to an ambient temperature of 115°F. At extremely high temperatures, skin blood flow can comprise over fifty percent of the cardiac output. (Roddie, 1983)

When exercise is performed in hot environments, even at moderate levels, problems with maintaining adequate blood flows to both muscles and skin occur. Compensations for these problems are similar to the compensatory actions that take place during more severe exercise under cool conditions, but they are usually encountered more quickly since skin blood flow is already increased dramatically by the heat stress. Typically, the maximum skin blood flow attainable at high levels of exercise and/or high ambient temperatures is between 7 and 8 L/min. (Rowell, 1974)

When exercising in a cool environment, skin blood flow remains low initially and cutaneous veins refill very slowly after muscles compress them during the action of exercise. This moves the majority of the skin blood volume to the central (core) regions and helps to maintain stroke volume and pressures. This is not the case when exercising in the heat. Muscles still compress cutaneous veins, but they refill so rapidly that the result is not as effective in displacing blood centrally. (Rowell, 1983)

In our model, we have attempted to describe these effects by combining five control relations with mass and energy balances and empirical relations for oxygen and carbon dioxide dissociation curves. To model the increase in muscle blood flow during exercise, we have used a proportional controller based on oxygen concentration in the blood leaving the muscles. Skin blood flow is controlled as a linear function of core temperature. Evaporative heat loss, through sweating, is based on an empirically derived linear controller which includes both core and skin temperature contributions.(Wyndham and Atkins, 1968) Blood flow to internal tissues is allowed to decrease to a minimal level to simulate repartitioning effects. This change occurs before cardiac output begins to increase. Since the typical thermal comfort zone for core temperature ranges between 36.6 and 37.1°C (Astrand and Rodahl, 1977), we have also set a controller in our model to automatically increase muscle metabolism when core temperature falls below 36.6°C. This is used to simulate the shivering response. Ventilation control is based on the chemoreflex control model of Duffin (1972).

This model has been developed on Matlab using the Simulink modeling package on a DEC Station (Model 2100) workstation. The equations were solved using a fifth order Runge-Kutta method available in Simulink.

REFERENCES

1. Astrand, Per-Olof and Kaare Rodahl. Textbook of Work Physiology: Physiological Bases of Exercise, Second Edition, McGraw-Hill Book Company, 1977. p. 529.

2. Duffin, J. *A Mathematical Model of the Chemoreflex Control of Ventilation. Respiration Physiology.* 15: 277-301. 1972
3. Ekelund, Lars-Goran. *Circulatory and Respiratory Adaptation during Prolonged Exercise.* ACTA Physiol. Scand. Suppl. 292. 1967.
4. Leigh, J. *Dynamic Mathematical Models of the Interaction Between the Thermoregulatory System and the Chemical Respiratory Control System in Mammals*, in Thermal Physiology, ed. J. R. S. Hales, Raven Press, 1984. pps. 359-364.
5. Mitchell, John W. *Energy Exchanges During Exercise*, in Problems with Temperature Regulation during Exercise, ed. Ethan R. Nadel, Academic Press Inc., 1977. pps. 11-26.
6. Nadel, Ethan R. *Circulatory and thermal regulations during exercise.* Federation Proc. 39: 1491-1497. 1980.
7. Nadel, Ethan R. *Effects of Temperature on Muscle Metabolism*, in International Symposium on Biochemistry of Exercise, eds. H. G. Knuttgen, J. A. Vogel, and J. Poortmans, Champaign, IL: Human Kinetic Publ., 1983. pps. 134-143.
8. Nadel, Ethan R., Enzo Cafarelli, Michael F. Roberts, and C. Bruce Wenger. *Circulatory regulation during exercise in different ambient temperatures.* J. Appl. Physiol. 46(3): 430- 437. 1979.
9. Nadel, E. R., S. M. Fortney, and C. B. Wenger. *Circulatory adjustments during heat stress*, in Exercise Bioenergetics and Gas Exchange, eds. Paolo Cerretelli and Brian J. Whipp, Elsevier/North-Holland Biomedical Press, 1980. pps. 303-313.
10. Roddie, Ian C. *Circulation to Skin and Adipose Tissue*, in Handbook of Physiology. Section 2: The Cardiovascular System. Volume III: Peripheral Circulation, Part 1, eds., John T. Shepherd and Francois M. Abboud, American Physiological Society, 1983. Chapter 10, pps. 285-318.
11. Rowell, Loring B. *Cardiovascular adjustments to thermal stress*, in Handbook of Physiology. Section 2: The Cardiovascular System. Volume III: Peripheral Circulation, Part 2, eds., John T. Shepherd and Francois M. Abboud, American Physiological Society, 1983. Chapter 27, pps. 967-1023.
12. Rowell, Loring B. *Competition Between Skin and Muscle for Blood Flow During Exercise*, in Problems with Temperature Regulation during Exercise, ed. Ethan R. Nadel, Academic Press Inc., 1977. pps. 49-76.
13. Rowell, Loring B. *Human Cardiovascular Adjustments to Exercise and Thermal Stress.* Physiological Reviews. 54(1): 75-159. 1974.
14. Saltin, Bengt. *Circulatory Adjustments and Body Temperature Regulation During Exercise*, Chapter 23 in Physiological and Behavioral Temperature Regulation, eds. James D. Hardy, A. Pharo Gagge, and Jan A. J. Stolwijk, Charles C. Thomas, 1970. pps. 316-323.
15. Saltin, Bengt. *Circulatory response to submaximal and maximal exercise after thermal dehydration.* J. Appl. Physiol. 19(6): 1125-1132. 1964.
16. Wyndham, C. H. and A. R. Atkins. *A Physiological Scheme and Mathematical Model of Temperature Regulation in Man.* Pflugers Arch. 303: 14-30. 1968.

APPENDIX 3

Availability Analysis of an Air Recovery System

Caroline K. Wilharm
Department of Chemical Engineering
Iowa State University
Ames, IA 50011

The objective of this project is to construct a model of a life support air recovery system (ARS) in order that the energetic and entropic characteristics of its components may be examined, and an entropically "optimal" system may be designed. The model consists of a closed loop of processing equipment based on standard data and specifications[1], mass and energy balances, and calculation of lost work. It is constructed so that inputs to the system (diet, activity level) as well as the operating conditions for each of the components may be varied, and new values for product masses, energy loss and lost work may be computed. This allows comparison of different scenarios and conditions, which can lead to optimization.

General Set-up:

The model can be broken down into three parts: the air recovery system, connected systems, and externals. Figure 1. is a schematic of how these are linked together.

The air recovery system is the largest, most extensive portion. It can be divided into subsystems which perform a specific task in achieving the goal of the ARS, the conversion of carbon dioxide, a product of respiration, into oxygen, an essential for sustaining life. The first subsystem separates CO_2 from air, the second converts this CO_2 into methane or carbon and water by reaction with hydrogen, and the final is electrolysis of water into hydrogen and oxygen.

The connected systems are in place to provide for the ARS, and to make the system closed. The cabin provides all of the air to be processed to the ARS. The urine processing system and air-conditioning systems are in place to recover water leaving the cabin and feed it back into the water reservoir for electrolysis. Air-conditioning also maintains the cabin temperature. A solar cell is included as a source of electricity for the entire

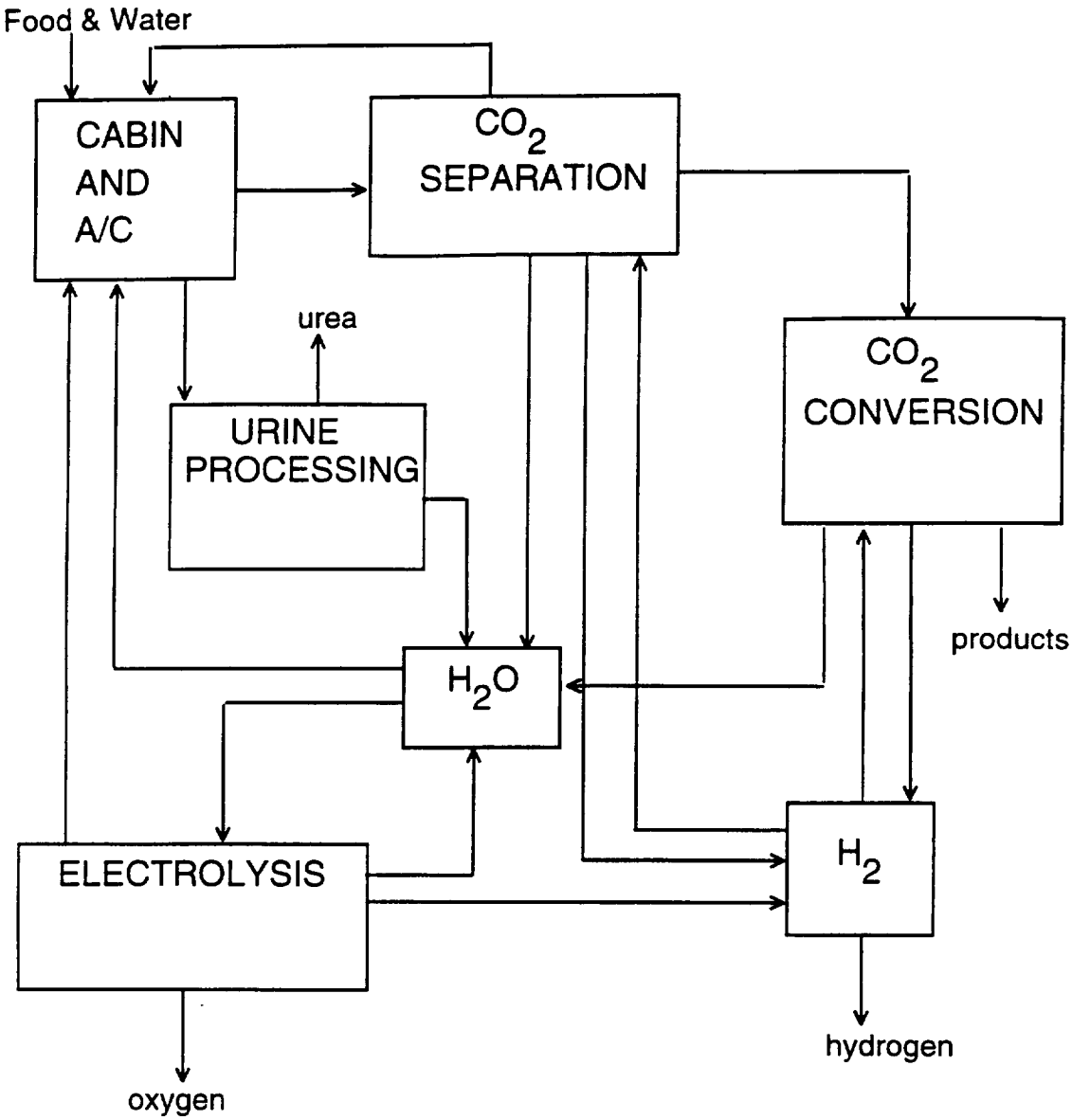

Figure 1. Simplified schematic of air recovery system, including cabin and urine processing subsystems.

system. A refrigeration system provides cooling water for heat exchange to the entire system.

Conservation Equations:

The system is required to meet the conservation laws. Mass and energy must be conserved, and entropy may only be generated, not destroyed. Based on these principles, balance equations may be written for the system as a whole, each of the subsystems, as well as each piece of equipment or reservoir in the loop. Species mass balances are of the form:

$$dm_i = \Sigma w_{ij}\delta_j + \Sigma \nu_{ik} M_i d\xi_k$$

The mass of species i accumulated in the system is equal to the sum of the masses of species i flowing in and out of the system plus the net generation of species i by reaction. The entire system is assumed to be at steady state, so no mass is accumulated in the system, and the left-hand side of the equation drops out.

The energy balances are quite simplified and based on the following assumptions. Changes in kinetic and potential energy are assumed negligible, gases and mixtures are assumed ideal. This yields energy balances of the form:

$$\Sigma\Sigma H_{ij} w_{ij}\delta_j + \Sigma\Delta H_{rk} d\xi_k = Q - W_s$$

The energy flowing out of the system minus the that flowing in plus energy generated by reaction is equal to the heat accumulated in the system minus the work done by the system on the surroundings. The shaft work for an ideal gas is derived from the integral of VdP for a reversible isothermal process and is given as:

$$W_s = -RT_o \ln(P_{out}/P_{in})/\eta$$

T_o is the system reference temperature and η is an efficiency which accounts for irreversibilities in the system. For an incompressible liquid, the shaft work is given as:

$$W_s = \Delta P/\rho\eta$$

ρ is the density, assumed constant.

Lost work is a measure of irreversibilities in the system. It is defined as the work which could ideally be done by the system minus the work actually done by the system. It is quantified by an entropy balance:

$$W_l = T_o diS = To\Sigma\Sigma S_{ij} w_{ij} \delta_j + T_o \Sigma \Delta S_{rk} d\xi_k - Q$$

The entropy generated is equal to the flow of entropy out minus the flow in plus entropy generated by reaction minus the energy accumulated divided by the reference temperature. The entropies are corrected for deviation from reference pressure by $-Rln(P/P_o)$, and there is an entropy correction for mixing of species, $RSx_i lnx_i$. Since entropy may only be generated and not destroyed, lost work is always a positive number, and may equal zero for a completely reversible system.

Model Framework:

The model consists of a series of calculations. The first section is a model of metabolism based on diet and activity level. The oxygen consumption, the amount of carbon dioxide and water produced in respiration, and the amount of urine and sweat are first determined. Next, the amount of gases leaving the cabin is computed based on set mole fractions of nitrogen, oxygen, carbon dioxide and water vapor, and the amount of carbon dioxide respired.

The next section is a series of mass balances on each of the system components. Mass balances on the cabin determine the amount of oxygen sent to storage, and the amount of nitrogen to be replenished. A mass balance on the water reservoir determines the amount of water to be sent to the electrolysis subsystem, and a balance on the hydrogen reservoir yields the amount of hydrogen to be sent to storage. The other mass balances determine the mass flows to the next piece of equipment in the loop, as well as the amounts of any products of reaction or trace gases vented to the surroundings.

The next section is a series of energy balances on each of the pieces of equipment. Prior to the energy balances, heats and entropies of reaction are computed, as well as any electrical requirements. These values are needed in the energy and lost work calculations to follow. The energy balances yield the amount of energy accumulated in the system. Since steady state is assumed for the system mass balances, it follows that energy also, should not accumulate in the system. It is assumed that no en-

ergy is lost through the walls of the equipment and thus, energy must be carried out of the system by heat exchange with another medium. The values of Q from the energy balances are used to determine the mass flows of the heat exchange medium from an energy balance on the medium. Most of the equipment operates exothermically and thus requires cooling water. A few of the pieces require energy, and in these cases energy is provided from streams internal to the system.

The next major section is the calculation of lost work for each piece of equipment. The equations used here are slightly different than given above, in that Q is now equal to zero and the entropy of the flow streams includes the heat exchange streams. Finally, an energy balance on all of the cooling water allows for the design of the refrigeration subsystem, and determination of the total electrical requirement allows design of a solar cell. As a final step the lost work for these subsystems is computed.

Base case:

The system modeled here is fairly complex and there are many subtleties involved in the model equations. One of the goals of this project is to compare results for different operating conditions and activity levels. The level of complexity of the system lends itself to a fairly conservative approach in making such comparisons. Before such efforts are undertaken, it is important to fully understand the case to which all comparisons will be made. After a firm grasp of the base case is achieved, then systematic variation of parameters may be undertaken.

The base case is for a single person at rest in the cabin at 299 K, 1 atm. These are the reference temperature and pressure for the entire system. The air conditioning system consists of a heat exchanger which maintains the cabin temperature, and a condenser external to the cabin, which removes water from the air leaving the cabin. This condenser operates isothermally, and water is condensed by compression of the air stream. The efficiency of the compressor may be varied. All condensations are based on Henry's law. This means that a trace of water remains in the gas phase and a trace of uncondensable gases will remain in the liquid phase.

The urine processing system consists of an evaporator supplied with electrical energy which separates water cleanly from urea with variable efficiency. The urea and unevaporated water are discarded as waste, and the evaporated water is condensed by cooling and sent to the water reservoir.

Air leaving the A/C condenser is sent to the CO_2 separation subsystem, shown in Figure 2. The separation itself occurs in an electrochemical depolarized carbon dioxide concentrator (EDC) [2]. The net reaction is

$$CO_2 + 1/2O_2 + H_2 \text{ ---> } CO_2 + H_2O + \text{electricity} + \text{heat}$$

A stoichiometric amount of hydrogen is fed to the reactor based on the mass of carbon dioxide in the air stream. The reaction occurs at constant pressure, the electricity liberated is directly usable by other components, and the extent of reaction may be varied. The unreacted hydrogen is sent back to the hydrogen reservoir after being cooled back to reference temperature through a heat exchanger. The nitrogen and unreacted oxygen is sent back to the cabin after heat exchange. The carbon dioxide and water vapor is sent to a condenser which cools the mixture isobarically to it's saturation temperature. The condensed phase is sent to another heat exchanger where it is further cooled to T_o and the gas stream enters the CO_2 conversion subsystem.

CO_2 conversion is achieved by reduction in the presence of hydrogen. There are two common reactions, Bosch and Sabatier, which require different types of reactors, conditions and supporting equipment, so the subsystems are quite different. Models for both have been developed.

The Bosch system(Fig. 3.) involves the reaction

$$CO_2 + 2H_2 \text{ ---> } C + 2H_2O + \text{heat}$$

A recycle reactor is used since the single-pass conversion of CO_2 is very low. In the model, the recycle ratio is variable, as is the single-pass conversion. A stoichiometric amount of hydrogen is mixed with the CO_2/water stream from the separation subsystem, and heated to the reaction temperature in the feed exchanger. A portion of the reactor product stream is used as the heat source. The feed stream is then compressed isothermally to the reaction pressure and sent to the reactor. The reactor operates at constant pressure and products are allowed to reach a set temperature. Carbon is removed from the reactor and the vapor product stream is sent to a heat exchanger where it is cooled at constant pressure. The cooled stream is compressed isothermally, water is condensed out, and the vapor phase is split. A fraction is recycled, the rest is vented. The liquid stream is sent to the water reservoir. The recycle stream is heated

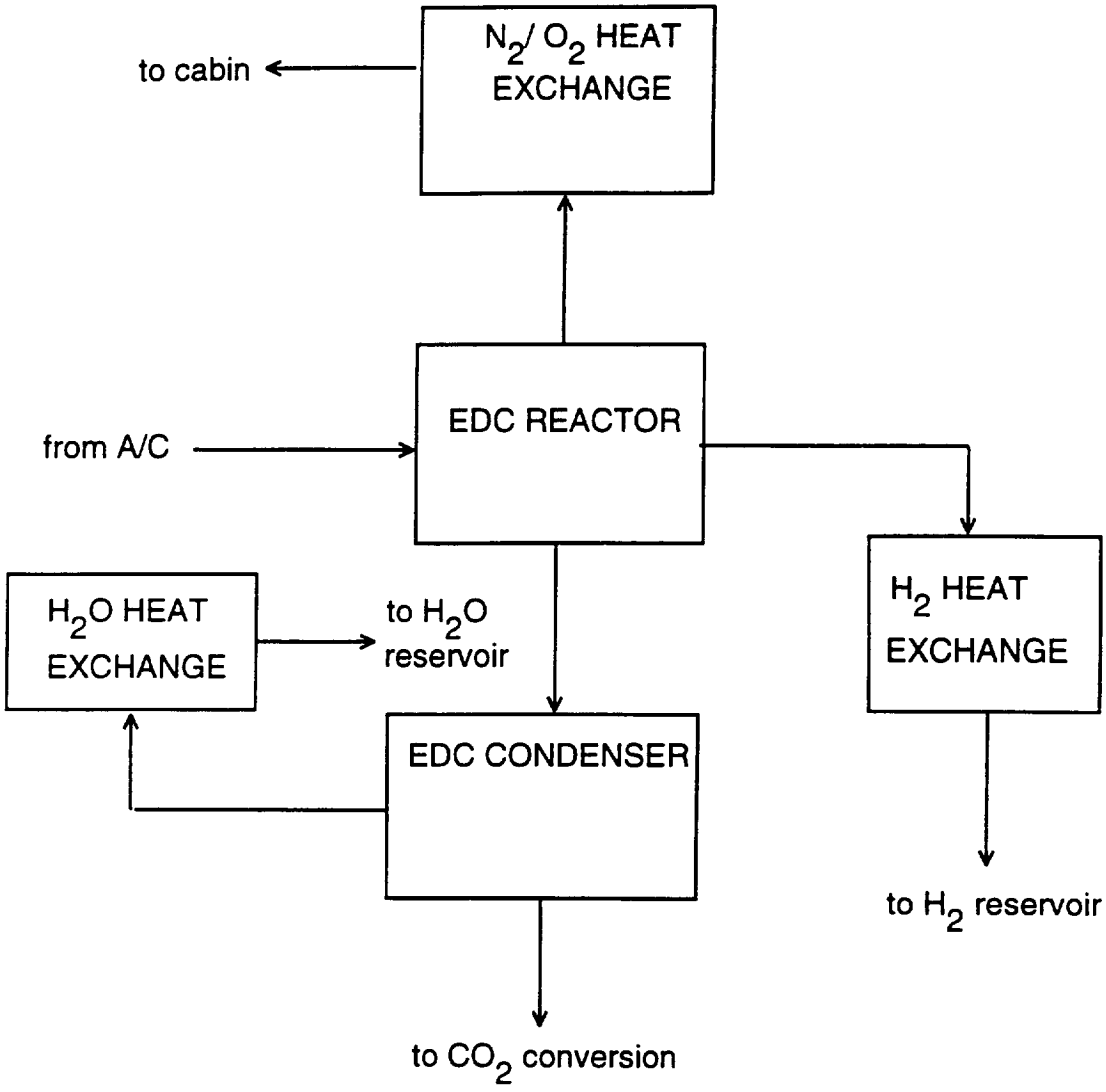

Figure 2. CO2 separation subsystem.

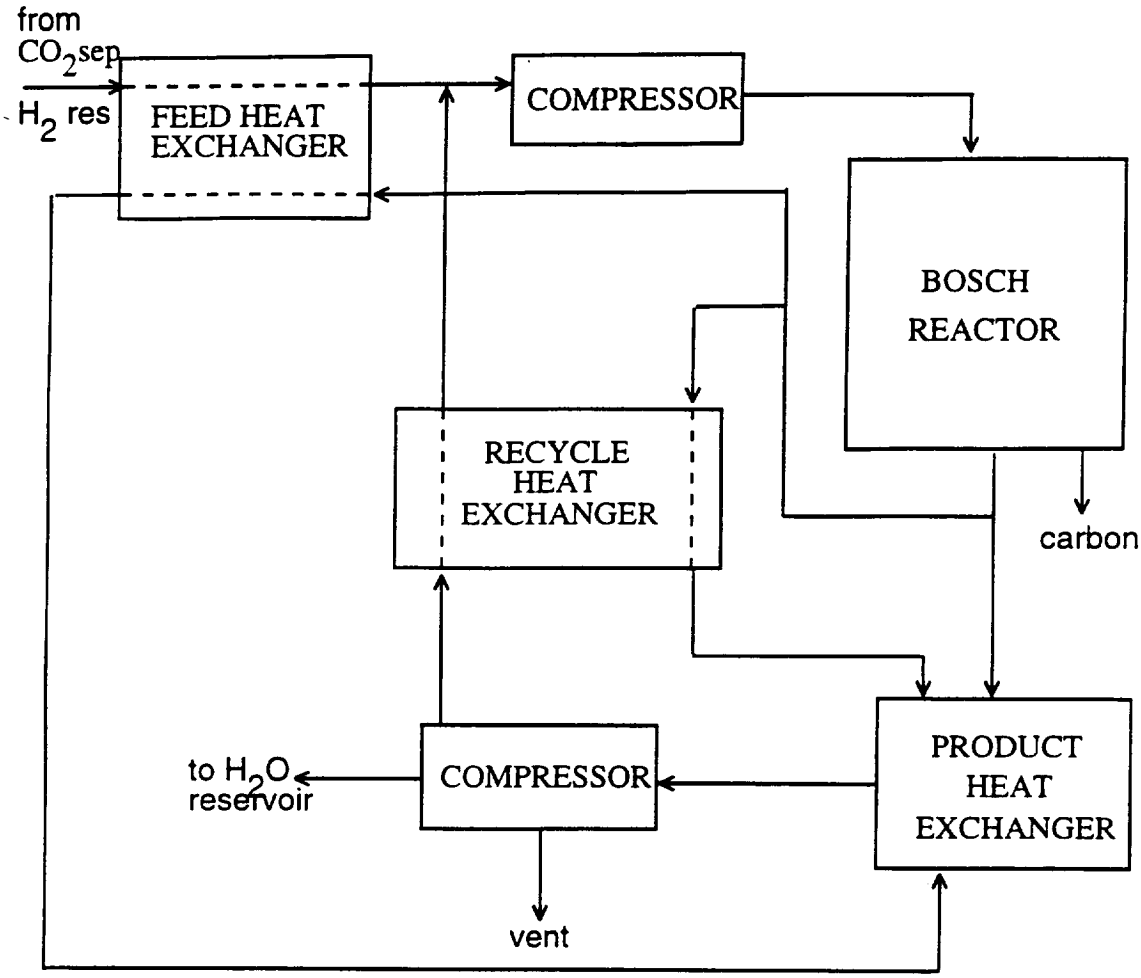

Figure 3. Bosch CO2 conversion subsystem.

to the reaction temperature and expanded to the reaction pressure. This exchanger also uses a portion of the product stream as a heat source.

The Sabatier subsystem(Fig. 4.) involves the reaction

$$CO_2 + 4H_2 \text{ ---> } CH_4 + 2H_2O + \text{heat}$$

The conversion for this reaction is high, so recycle isn't necessary. Similarly, a stoichiometric amount of hydrogen is mixed with the vapor stream from the separation system and heated to reaction temperature. A fraction of the product stream is used as a heat source. The feed is compressed isothermally to the reaction pressure and sent to the reactor. The reaction occurs at constant pressure and allowed to reach a set temperature. Unreacted hydrogen leaves the reactor, is cooled at constant pressure, allowed to expand to atmospheric pressure and is sent back to the hydrogen reservoir. The product stream is cooled isobarically to the reference temperature in a heat exchanger, and then compressed isothermally to condense the water. This process is somewhat of a black box because the separation of methane occurs spontaneously here, as does the separation of unreacted hydrogen in the reactor. Methane is stored, the liquid phase is sent to the water reservoir, and the methane-free vapor phase is vented.

The electrolysis subsystem (Fig. 5.) is designed to convert all of the metabolic water, except what is needed to maintain cabin humidity, into oxygen and hydrogen. Water is sent from the water reservoir to a heat exchanger where it is heated at constant pressure to the reaction temperature, and then compressed isothermally to the reactor pressure. Heat is supplied to the exchanger by the one of the product streams. The electrolysis unit is a solid polymer water electrolysis subsystem[3]. The net reaction is

$$\text{electricity} + H_2O \text{ ---> } 1/2O_2 + H_2 + \text{heat}$$

The conversion for this reactor is very low, so a large surplus of water is cycled through in order to convert all of the metabolic water into products. Pure oxygen exits one side, is cooled in a heat exchanger and expanded to atmospheric pressure. The oxygen needed to replenish the cabin is sent there, the remainder is sent to storage. Liquid water and hydrogen exit and are cooled at constant pressure. Water and hydrogen spontaneously separate cleanly in the exchanger, the water returns to the water reservoir, the hydrogen is expanded to atmospheric pressure and sent to the hydrogen reservoir.

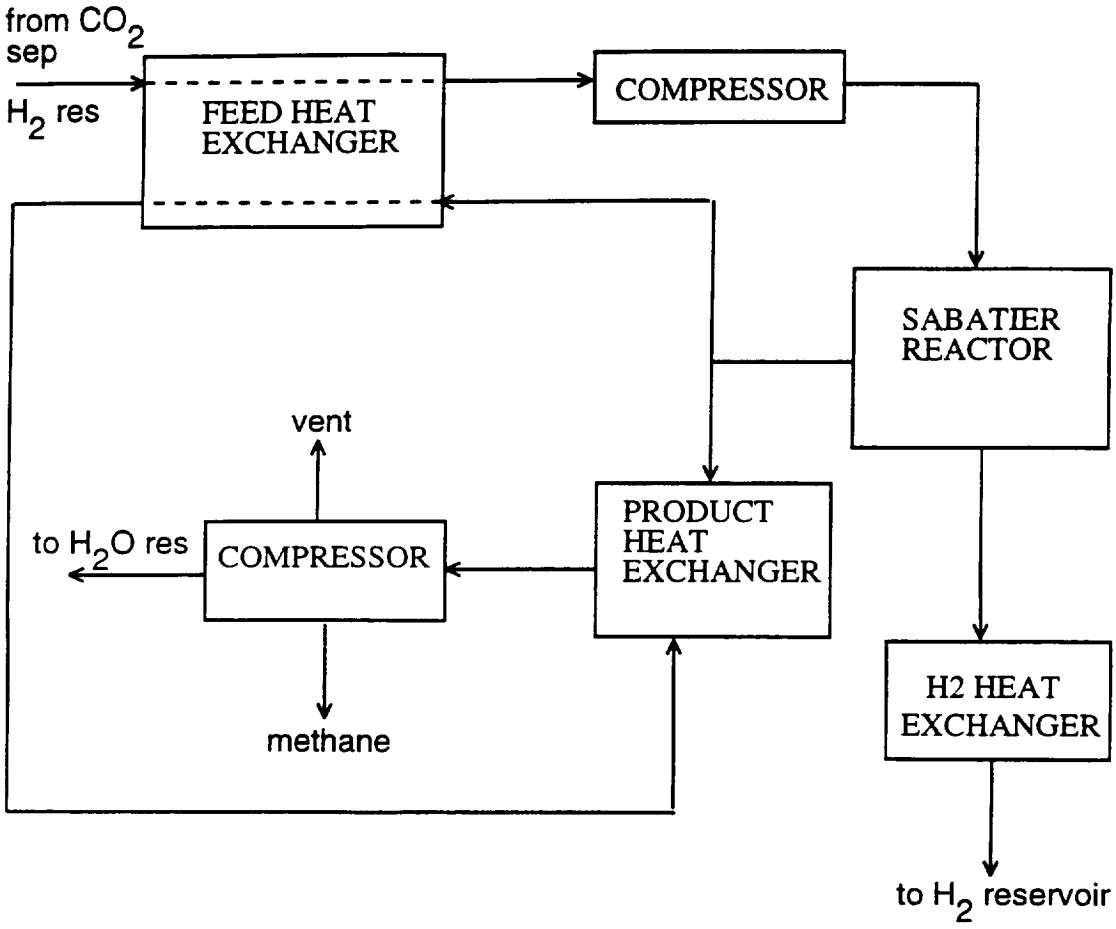

Figure 4. Sabatier CO2 conversion subsystem.

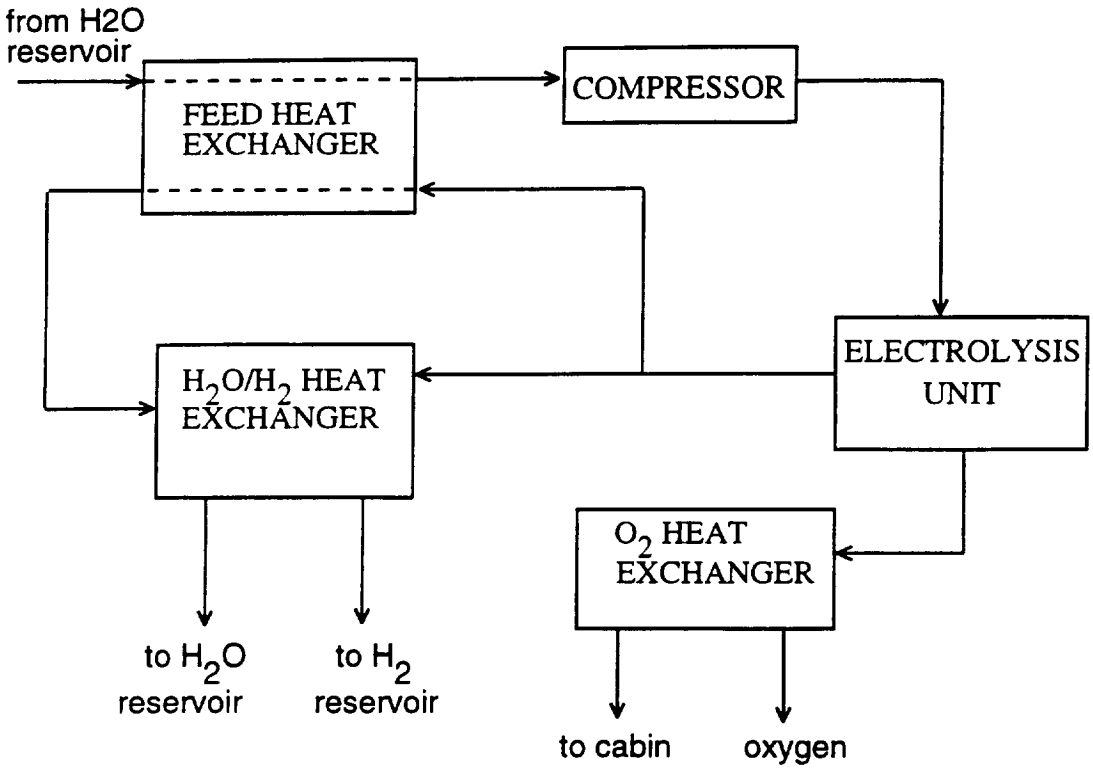

Figure 5. Electrolysis subsystem.

The refrigeration system handles all of the cooling water for the components described above. The refrigerator operates as a vapor-compression cycle[4]. Cooling water circulates through an evaporator where it undergoes heat-exchange with Freon-12. The Freon is compressed, then condensed at constant pressure by radiative heat exchange. The Freon is then expanded isenthalpically to its initial state to complete the cycle.

Electricity is supplied to the system by a solar cell [5]. This cell is somewhat of a black box, whose size is determined by demand, and efficiency is dependent on temperature. The design equations are based on the assumption that the sun, surroundings and the cell radiate as black bodies and that the cell is a flat square sheet of negligible thickness which absorbs radiation from the sun on one face, radiates to and absorbs radiation from the surroundings on both faces, and exchanges heat with the system on one edge.

Results:

Table 1. shows the operating conditions and results of the mass, energy and lost work calculations for the base case with the Bosch CO_2 conversion subsystem. Table 2. shows the same for the Sabatier subsystem. Comparison of the tables shows that the mass flows, net heat, cooling requirement and lost work are identical for the two scenarios up to the conversion subsystem, as should be for identical equipment and conditions. The Bosch subsystem has a net positive energy and higher cooling water requirement and lost work than the Sabatier subsystem. Since a system with fewer irreversibilities is favorable, the Sabatier subsystem with its lower lost work is more desirable. However, because of the higher conversion of the Sabatier subsystem, more water is produced and sent to electrolysis, raising the cooling requirement and lost work for the electrolysis subsystem. Since the electrolysis subsystem is the greatest contributor to the net lost work for the ARS as a whole, the increase in lost work here due to increased flow greatly outweighs the increase in lost work incurred using Bosch instead of Sabatier. Also, increasing the flow through electrolysis will increase the amounts of hydrogen and oxygen sent to storage. Since the Bosch subsystem also provides a surplus of hydrogen and oxygen at a lower entropic cost, by that criterion, it can be said to be more desirable than Sabatier. Also, the refrigeration system for Bosch has a lower flow because of the decreased cooling requirement for electrolysis, and a solar cell of smaller area can be used because of the lower electricity requirement. This also brings down the total lost work.

Table 1. Bosch base case.

component	inlet T	outlet T	Pout/Pin	effncy/conv	power cons.	mass flow	Q	cooling req	lost work
	(C)	(C)			(J/min)	(g/min)	(J/min)	(mol/min)	(J/min)
cabin	26	26	1	-----	-----	67.9979	-3427	2.8408	63769
A/Ccondenser	26	26	3.294	0.8	-----	67.9979	-10671	14.1522	212134
CABIN - A/C						**NET**	**-14098**	**16.993**	**275903**
urine evap	37	373	1	0.8	7153	2.4174	5722	-----	11783
urine cond	373	26	1	-----	-----	2.2559	-5787	0.8528	609
URINE PROC.						**NET**	**-65**	**0.8528**	**12392**
EDC reactor	26	287	1	0.8	-36003	68.9665	-98513	1.8198	35303
EDC condense	287	46	1	-----	-----	14.4264	-40160	0.7468	468
N2/O2 heat	287	26	1	-----	-----	54.158	-13823	0.257	1130
H2 heat	287	26	1	-----	-----	0.3821	-1441	0.0268	117
H2O heat	46	26	1	-----	-----	14.0634	-2147	0.6087	17188
CO2 SEP'N						**NET**	**-155084**	**3.4591**	**54206**
feed exch	46	649	1	-----	-----	0.3962	536	-----	44
feed compr	649	649	1.273	0.8	-----	2.0844	-98	0.0014	5
Bosch	649	717	1	0.1	-----	2.0844	-255	0.0039	641
product heat	717	26	1	-----	-----	2.0326	-645	0.1057	2724
product comp	26	26	2.717	0.8	-----	2.0326	-721	0.9593	14414
recycle exch	26	649	1	-----	-----	1.6882	2314	-----	475
CO2 CONVRSN						**NET**	**1119**	**1.0703**	**18303**
electro exch	26	65	1	-----	-----	493.0369	80456	-----	3010
electro comp	65	65	7.797	0.8	-----	493.0369	-838	0.6945	15798
electrolysis	65	91	0.916	0.034	414278	493.0369	-87698	16.3814	1280754
O2 heat exch	91	26	0.14	-----	-----	14.8841	-889	0.1671	5607
H2/H2O heat	91	26	0.14	-----	-----	478.1528	-84976	36.4577	872821
ELECTROLYSIS						**NET**	**-63951**	**53.7007**	**2177990**
REFRIGERATOR	-----	10	1	0.8	-----		**-321110**	-----	**94704879**
	T source	T cell	T surround	efficiency	power	area	heat		lost work
	(K)	(K)	(K)		(J/min)	(sq m)	(J/min)		(J/min)
SOLAR CELL	6000	300	0	0.24	**386098**	19.7	**0**		**1708377**

Table 2. Sabatier base case.

component	inlet T	outlet T	Pout/Pin	effncy/conv	power cons.	mass flow	Q	cooling req	lost work
	(C)	(C)			(J/min)	(g/min)	(J/min)	(mol/min)	(J/min)
cabin	26	26	1	-----	-----	67.9979	-3427	2.8408	63769
A/Ccondenser	26	26	3.294	0.8	-----	67.9979	-10671	14.1522	212134
CABIN - A/C						**NET**	**-14098**	**16.993**	**275903**
urine evap	37	373	1	0.8	7153	2.4174	5722	-----	11783
urine cond	373	26	1	-----	-----	2.2559	-5787	0.8528	609
URINE PROC.						**NET**	**-65**	**0.8528**	**12392**
EDC reactor	26	287	1	0.8	-36003	68.9665	-98513	1.8198	35303
EDC condense	287	46	1	-----	-----	14.4264	-40160	0.7468	468
N2/O2 heat	287	26	1	-----	-----	54.158	-13823	0.257	1130
H2 heat	287	26	1	-----	-----	0.3821	-1441	0.0268	117
H2O heat	46	26	1	-----	-----	14.0634	-2147	0.6087	17188
CO2 SEP'N						**NET**	**-155084**	**3.4591**	**54206**
feed exch	46	177	1	-----	-----	0.4294	189	-----	168
feed compr	177	177	2.283	0.8	-----	0.4294	-32	0.0006	7
Sabatier	177	527	1	0.95	-----	0.4294	-479	0.0784	3168
product heat	527	26	1	-----	-----	0.4261	-926	0.1613	7167
product comp	26	26	2.567	0.8	-----	0.4261	-24	0.0317	475
H2 heat exch	527	26	0.779	-----	-----	0.0033	-24	0.0005	10
CO2 CONVRSN						**NET**	**-1355**	**0.2725**	**10995**
electro exch	26	65	1	-----	-----	496.7486	81062	-----	3033
electro comp	65	65	7.797	0.8	-----	496.7486	-844	0.6997	15916
electrolysis	65	91	0.916	0.034	417396	496.7486	-88357	16.5048	1290395
O2 heat exch	91	26	0.14	-----	-----	14.9962	-901	0.1684	5649
H2/H2O heat	91	26	0.14	-----	-----	481.7524	-85539	36.7322	866401
ELECTROLYSIS						**NET**	**-64632**	**54.1051**	**2181394**
REFRIGERATOR	-----	10	1	0.8		0	**-316220**	-----	**93225342**
	T source	T cell	T surround	efficiency	power	area	heat		lost work
	(K)	(K)	(K)		(J/min)	(sq m)	(J/min)		(J/min)
SOLAR CELL	6000	300	0	0.24	390018	19.9	**0**		**1752892**

There is a considerable range of values for lost work for the individual pieces of equipment. Most of the lost work is in the refrigeration subsystem. This system is responsible for restoring all of the cooling water in the system back to its initial temperature. By reducing the temperature and entropy of high temperature, high entropy streams without making use of the available work, a great deal of work is lost. The next highest generator of lost work is the solar cell. This converts sunlight, with a very high availability, into electricity, of lesser, but still high availability. The high lost work is a result of the immense temperature difference between the source (6000 K), the surrounding space (0 K), and the operating temperature of the cell (300 K). In the same league as the solar cell, are the processes which consume electricity. Electricity has a high availability, and its degradation into heat, or work to drive electrolysis, is entropically expensive.

It is difficult to rank the remaining pieces of equipment by lost work without getting into the very specific details of each of the balance equations. However, there are general trends which can easily be discussed for each of the different types of equipment. The remaining equipment can be broken down into three categories: reactors, compressors, and heat exchangers. The reactors have inlet to outlet temperature differences, may have pressure differences and have changes in enthalpy and entropy associated with reaction. The cabin is considered a reactor because of the metabolic generation of heat. Of the reactors, the cabin has the greatest lost work. This is because of the mixing of streams, the evaporation of water, and metabolism. The EDC reactor is next, and would have a higher value were it not for the production of electricity. The Sabatier reactor follows, and the least lost work is for the Bosch reactor.

The compressors have a wide range of values. Since all of the equations here are of the same form, the lost work per unit of mass flow better shows the effects of the different conditions. The most lost work is for those compressions which involve a phase change. Also, the higher the pressure difference, the more lost work. The heat exchangers follow the same rationale; those involving phase change have more lost work, as well as do those with large temperature differences. Also, mixing of streams of different compositions will increase lost work.

Variations:

With an understanding of the base case, examination of the effects of changing operating conditions and activity level can have some meaning.

A change in activity level is achieved for the model by changing the respiratory quotient. This shifts the O_2/CO_2 ratio. Figure 6. illustrates the effect of increasing the respiratory quotient from resting to maximum activity on the energy, cooling water and lost work for the system. This shift causes the respiration rate to increase to 15-times resting level. Any ratio above 15 reflects the increased mass of carbon dioxide in the system. With the mass fractions of species exiting the cabin fixed, the total flow through the ARS will increase. The lost work for all the components of the ARS will change in proportion to the change in CO_2, with the exception of the electrolysis subsystem. The disproportionate change of water respired, sweat and in urine will alter the amount of water sent to electrolysis. This will change the amounts of hydrogen and oxygen sent to storage. The lost work for the cabin will not change proportionally since the oxygen flow into the cabin will change with the respiratory quotient, and, the metabolic heat changes with varying diet. Since the dietary requirement for different activity levels is based on increased carbohydrate consumption with fixed fat and protein consumption, the amount of urine produced will not change.

Another variation is to change the efficiency of the compressors. Lowering their efficiency increases lost work. The increase is not proportional to the efficiency change since the lost work for the flowing streams remains constant, only the shaft work input changes. Figure 7. shows the effect of efficiency on lost work for the air conditioning, electrolysis, Bosch and Sabatier subsystems. The cabin/A-C and Bosch subsystems are the most sensitive to efficiency since upwards of 75% of the lost work is contributed by the condensers at maximum efficiency. Less than 5% of the lost work is contributed by the compressors for the electrolysis and Sabatier subsystems at maximum efficiency.

The final simple variations are to change the extents of reaction for the reactors. Variation of the extent of reaction for the CO_2 conversion subsystem has an impact on the flows and lost work of the equipment downstream. Increased extent of reaction will increase the products and decrease the unreacted H_2 and CO_2. The decrease in unreacted hydrogen will change the amount of hydrogen sent to storage, and the increased amount of water produced will increase the amount of water sent to electrolysis, increasing the oxygen and hydrogen sent to storage. The main impact will be to change the energy, cooling water and lost work for the conversion subsystem itself, as the change in mass flow through equipment downstream is not enough to induce changes on the same order as

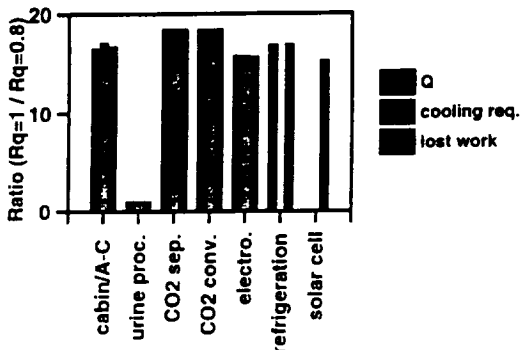

Figure 6. Effect of respiratory quotient on system.

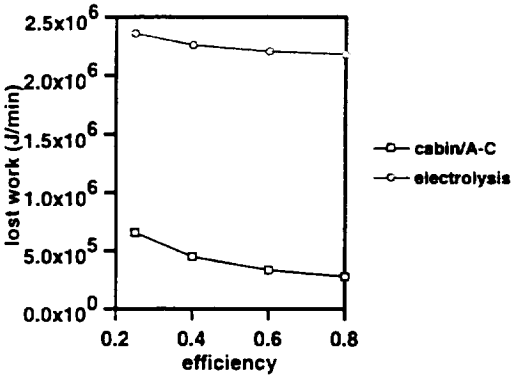

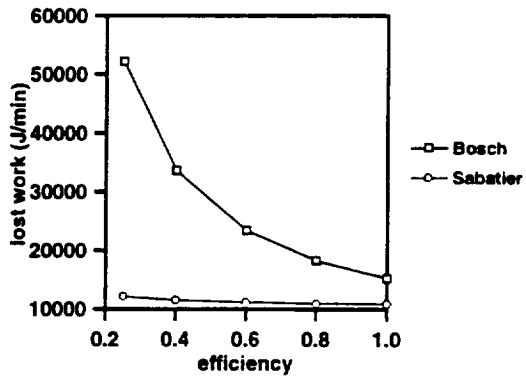

Figure 7. Effect of efficiency on lost work.

for this subsystem. Figure 8. shows the influence of extent of reaction on energy, cooling water and lost work for the Sabatier subsystem. These increase linearly with increased extent. Figure 9. shows the same for the Bosch subsystem. Overall conversion is also plotted since this is a recycle reactor. The same behavior is exhibited. Figure 10. shows the effects of changing the fraction of vapor from the product condenser which is recycled. The amount of lost work increases more rapidly than the energy and cooling water.

Figure 11. shows the effect of decreased extent of reaction for the EDC reactor on the system as a whole. The energy, cooling water and lost work for the subsystem exhibit the same linear behavior as changing the extent of reaction for the Sabatier reactor. However, the decrease in mass of CO_2 sent on to the rest of the system greatly affects the outcomes downstream. The graph compares values using the lower limit for conversion in the EDC reactor based on thermodynamic constraints set by the design of the system, to the values from the Bosch base case. Decreased extent decreases the separation of carbon dioxide, and the amounts of hydrogen and oxygen consumed, and the amount of water produced. This affects the amount of hydrogen and oxygen sent to storage. Values for the conversion subsystem increase because less water is produced in the separation process which will take less CO_2 out of the system when the product stream is condensed, sending more CO_2 to the conversion system. The subsequent subsystems have decreased values because less water is produced in the EDC reactor, so less water goes to electrolysis requiring less electricity, and less cooling water is needed for the system overall.

Figure 12. shows the effect of increased extent of reaction for electrolysis. Values using the upper limit for conversion set by thermodynamic design constraints are compared to those for the Bosch base case. Increased conversion decreases the values in this case because the surplus of water circulating is decreased. Varying the extent of reaction for the electrolysis unit also impacts the amount of hydrogen and oxygen sent to storage. The values for the solar cell and refrigeration subsystem are decreased because the requirements for the electrolysis subsystem are decreased, and these make up a substantial portion of the cooling and electrical demand for the system as a whole.

Other variations may be done. Operating temperatures and pressures may be varied. These variations would require changing the enthalpies and entropies in the model equations. This task is complicated by the pos-

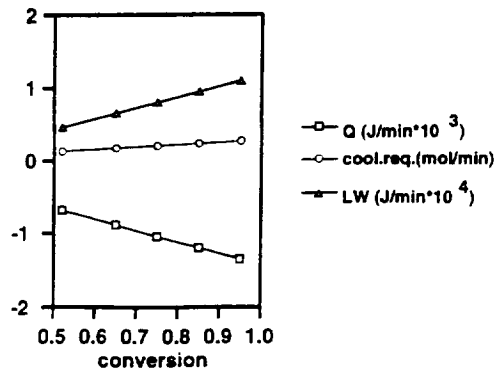

Figure 8. Effect of conversion on Sabatier subsystem.

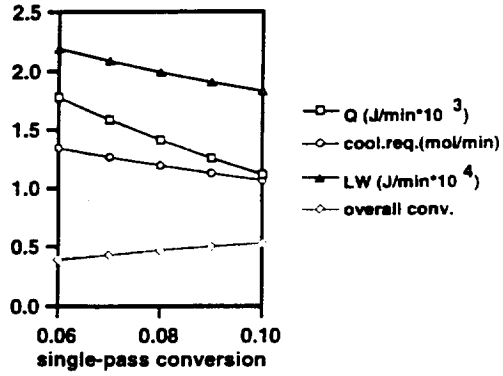

Figure 9. Effect of single-pass conversion on Bosch subsystem.

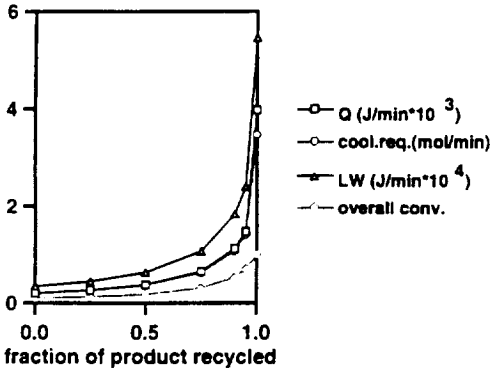

Figure 10. Effect of recycle fraction on Bosch subsystem.

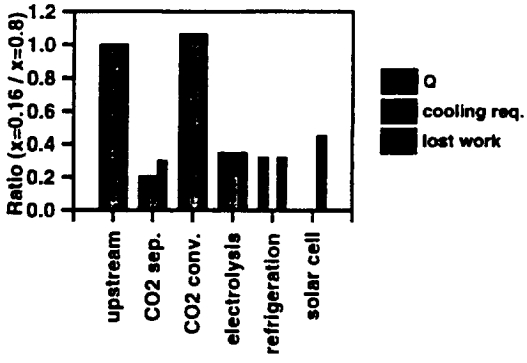

Figure 11. Effect of CO2 separation on system.

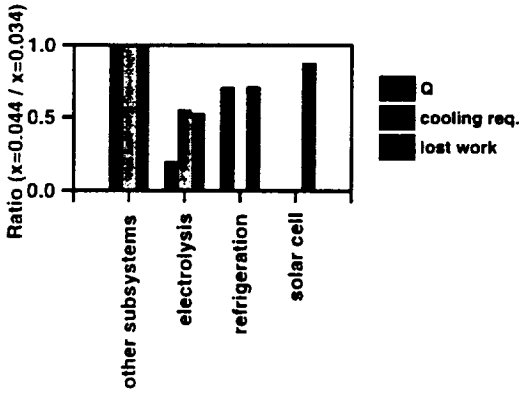

Figure 12. Effect of electrolysis conversion on system.

sibility of phase changes, so the operating conditions must be adjusted carefully to minimize changes in the model equations. Also, changes in pressures and temperatures, as well as the changes mentioned above, may lead to values for lost work that violate the laws of thermodynamics. Establishing limits for the operating conditions is mandate to understanding when the model is valid, and optimization. A great deal more work is necessary to establish these limits. Also, different types of equipment may be used in the model, and their operational limits and optima may be determined to find the optimum for the system as a whole.

References:

[1] Wydeven, Theodore, "A Survey of Some Regenerative Physico-Chemical Life Support Technology", NASA Technical Memorandum 101004, November 1988.

[2] Ibid., p 3.

[3] Ibid., p 8.

[4] Smith, J.M., and H.C. Van Ness, *Introduction to Chemical Engineering Thermodynamics*, 4th edition. McGraw-Hill, Inc., New York, 1987. pp. 276-283.

[5] Luque, A., G.L. Araujo, Physical Limitations to Photovoltaic Energy Conversion. Adam Hilger, New York, 1990. pp. 84-90.

Using Second Law Analysis to Predict the Efficiency of ECLSS Subsystems

Sharmista Chatterjee and R. C. Seagrave
Iowa State Univ.

ABSTRACT

The objective of this paper is to present an estimate of the second law thermodynamic efficiencies of the various units comprising an Environmental Control and Life Support Systems(ECLSS). The technique adopted here is based on an evaluation of the 'lost work' within each functional unit of the subsystem. Pertinent information for our analysis is obtained from a user interactive integrated model of an ECLSS.The model was developed using a chemical process simulator called ASPEN (Advanced System for Process Enginering). A potential benefit of this analysis is the identification of subsystems with high entropy generation as the most likely candidates for engineering improvements.

INTRODUCTION :

This work has been motivated by the fact that the design objective of a life support systems analyst should be the evaluation of existing ECLSS technologies not only the basis of the quantity of work needed for or obtained from each subsystem but also on the quality of work.

In a previous study Brandhorst [1] showed that the power consumption for a partially closed and a completely closed regenerable life support systems were estimated as 3.5 kw/individual and 10-12 kw/individual respectively. Considering the increasing cost and scarcity of energy resources, our attention is drawn to evaluate the existing ECLSS technologies on the basis of their energy efficiency. In general the first law efficiency of a system is usually greater than 50%, [2]. From literature, the second law efficiency is usually about 10%, [3]. The second law efficiency of the system indicates the percentage of energy degraded as irreversibilities within the proces. This offers more room for improvement in the design of equipment.

From another perspective, our objective is to keep the total entropy production of a life support system as low as possible and still ensure a positive entropy gradient between the system and the surroundings.The reason for doing so is as the entropy production of the system increases, the entropy gradient between the system and the surrounding decreases, and the system will gradually approach equilibrium with the surroundings until it reaches the point where the entropy gradient is zero. At this point no work can be extracted from the system. This is called as the ' dead state ' of the system, [4].

METHODS OF SECOND LAW ANALYSES :

The irreversibility or entropy generation within a process is evaluated on the basis of the second law of thermodynamics using two widely used techniques. These are:

- Availibility Analysis/Exergy Analysis
- Lost Work Analysis

Availibility analysis or exergy analysis is a widely used technique. This was first proposed by Guoy and Stodola [5,6]. Availibility is a measure of the useful work potential of a stream which is at a different state from the environment. This concept has been extensively used in determining the efficiency in areas ranging from space heating to cryogenic processes, [7,8].

The method of Lost Work Analysis was first proposed by Seader [9].

For our study we chose the lost work approach as it provides a more intuitive feeling for the irreversibilities within a functional unit.

CONCEPT OF LOST WORK ANALYSIS :

The basic requirement of the second law is :

The total entropy change of an isolated system,

$$\Delta S_{sys} \geq 0.0 \qquad (1)$$

For a control volume with a steady state process where the surroundings are at a temperature of T_0, the

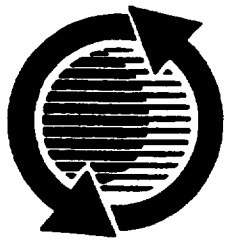

ISSN 0148-7191

Printed in USA

90-1203B/PG

rate of change of the total entropy of the system is given by, [10]

The rate of change of total entropy of the system	=	Net rate of entropy transfer by flowing streams	+	Rate of entropy exchange with the surroundings by heat transfer

Thus

$$\Delta(Sm)_{fs} - \frac{Q}{T_0} > 0.0 \qquad (2)$$

where $\Delta(Sm)_{fs}$ is the difference in entropy between the feed and the product and Q is the net heat transfer from the system to the surroundings

For a steady state flow process there is no internal energy accumulation within the system. The law of conservation of energy can be expressed as

$$\Delta\left[\left(H + \frac{1}{2}u^2 + zg\right)\right]_{fs} = Q - W_s \qquad (3)$$

where $\Delta\left[\left(H + \frac{1}{2}u^2 + zg\right)\right]_{fs}$ is the difference in energy between the inflow and the outflow streams.
Q is the heat flow into the system
W_s is the work done by the system

For any system which requires work, the amount of work required will be a minimum if the system undergoes a reversible change. This minimum work required is called the " ideal work ", (W_{ideal}). Since there is no degradation of work the entropy generation for a reversible process is equal to zero and equation (2) then becomes

$$Q = T_0\,\Delta(Sm)_{fs}$$

Substituting the above relationship in equation (3) and rearranging gives

$$W_{ideal} = T_0\,\Delta(Sm)_{fs} - \Delta\left[\left(H + \frac{1}{2}u^2 + zg\right)\right]_{fs} \qquad (4)$$

In most processes the kinetic and potential energy terms are negligible, and equation (4) can be written as

$$W_{ideal} = T_0\,\Delta(Sm)_{fs} - (\Delta H)_{fs} \qquad (5)$$

It is justified to mention here that from an availibility viewpoint, according to the defination of W_{ideal} as given in (5), the minimum work required is equivalent to the difference in availibility between the input and the output streams.

For a work producing process, the "lost work" is the work which is lost due to irreversibilities within the process. It is expressed as the difference between the ideal work which could be produced by the process (W_{ideal}) and the actual work produced by the process (W_s). Thus from equations (3) and (5), W_{lost} can be written as

$$W_{lost} = T_0\,\Delta(Sm)_{fs} - Q \qquad (6)$$

Conventionally, there are two kinds of processes. A spontaneous process is one which produces work, i.e W_{ideal} is positive. Then

$$W_s = W_{ideal} - W_{lost} \qquad (7)$$

A nonspontaneous process is one which requires some form of external work to be supplied, i.e Wideal is negative. Hence

$$|W_s| = |W_{ideal}| + W_{lost} \qquad (8)$$

Thereby the second law efficiency for each type of process can be defined as

$$\eta_2 \text{ (spontaneous process)} = \frac{W_s}{W_{ideal}} \qquad (9)$$

$$\eta_2 \text{ (nonspontaneous process)} = \frac{W_{ideal}}{W_s} \qquad (10)$$

METHODOLOGY ADOPTED :

The following steps were performed to evaluate the lost work and second law efficiency of each subsystem of an ECLSS based on the above developed concepts :

- Defining the subsystem boundary of the ECLSS subsystem chosen, i.e identifying the input and output streams for the chosen subsystem.
- Choosing the reference temperature. For our study we chose the space craft cabin temperature of 70°F.
- Evaluating the W_{lost} within each functional unit of the ECLSS subsystem.
- Calculating the W_{ideal} for each subsystem depending on the subsystem information provided.
- Evaluating the second law efficiency, knowing W_{lost} and W_{ideal}.

It is to be noted that, in order to calculate W_{lost} and W_{ideal}, detailed information about the input and output streams is required, i.e enthalpy, entropy and mass flow rate. To obtain the necessary data we developed a psuedo steady state model of the ECLSS using a state of the art chemical process simulator called ASPEN (Advanced System for Process

Engineering). The underlying feature of our model is that the inputs to the ECLSS subsystems are regulated by a user interactive model of the crew in the space craft. The crew model is appended to the main ASPEN code. Given the general crew specificattions like age, weight, gender, and activity level the crew model can compute the mass flow rates of different waste streams from the crew. These streams then serve as inputs to the ECLSS.

RESULTS :

A conventional ECLSS consists of the following subunits [11] :

- Solid waste management
- Humidity condensate removal
- Trace removal subsystem
- CO_2 reduction subsystem
- CO_2 removal subsystem
- O_2 generation subsystem
- Water recovery subsystem

Presented herein are the results obtained for a few sample technologies which are commonly in use in an ECLSS design.

WET OXIDATION OF SOLID WASTE :

The solid waste is oxidized in an autoclave at a pressure of 1067 psia in the presence of water,[12]. The reaction temperature depends on the carbon content of the feed and is usually between 100 and 374 °C. For our modeling purposes, we assume that only the carbon content of the feed is oxidized.

For the ASPEN model, the reactor is modeled using a RSTOIC block as shown in Figure 1. The reactor temperature is set according to the carbon content of the feed using the linear relationship as given by Takahashi [12]

$$\% \text{ of carbon in feed} = -0.65 \times \text{oxidation temperature} + 194 \qquad (11)$$

where oxidation temperature is the temperature which is to be maintained in the reactor.

The mass and energy balance information of the streams involved in the process is shown in Table1. It is to be noted that all these values are for a base case of a crew consisting of 1 man of age 25 years weighing 60 kg resting at basal metabolic rate.

Table 1: Properties of streams involved in solid waste wet oxidation subsystem.

Stream	Mass flow rate (lb/hr)	Total enthalpy (Btu/hr)	Total entropy (Btu/hr°R)
S1	3.44×10^{-4}	12.91×10^{-4}	23.56×10^{-7}
S2	9.16×10^{-4}	-1.4×10^{-3}	-2.64×10^{-3}
S3	1.26×10^{-3}	–4.77	-3.63×10^{-6}
S4	1.26×10^{-3}	–4.85	1.72×10^{-5}
S5	0	0	0
Q1	Heat duty = -4.77 Btu/hr		
Q2	Heat duty = -0.08 Btu/hr		

The lost work analysis of each unit operation block comprising the solid waste oxidizer is given in Table 2.

Table 2: Lost work estimation of the solid waste wet oxidation subsystem.

Unit operation block	Lost Work (Btu/hr)	% of total lost work
Wet oxidizer	4.71	98.1
Depressurizer	0.091	1.9
Total lost work	4.801	

$$W_{ideal} = 530\,(\,1.72\times10^{-5} + 2.64\times10^{-3} - 23.56\times10^{-7}) - (\,-4.85 - 12.91\times10^{-4} + 14.05\times10^{-4})$$

$$= 6.26 \text{ Btu/hr}$$

W_{ideal} being positive, this is a spontaneous process. Hence

$$W_S = 6.26 - 4.801$$
$$= 1.459 \text{ Btu/hr}$$

$\eta_2 = \frac{1.459}{6.26}$

= 23.3 %

CATALYTIC OXIDATION OF CONTAMINANT GASES :

The catalytic oxidation process is chosen for trace contaminant removal. This design was proposed by Ammann, [13]. In this subsystem, the incoming trace gas is split into two fractions depending on its methane content (i.e higher the methane content, the greater the volume of gas which goes into the high temperature oxidizer). One portion of the incoming trace gas is oxidized in a high temperature catalytic oxidizer (HTCO) which is maintained at a temperature of 400 - 450 °C. Prior to entering the HTCO the gas is heated in an electric heater. Remaining portion of the gas is oxidized in a low temperature catalytic oxidizer (LTCO) which is maintained at ambient temperature of 70 °F. The ASPEN model of this subsystem is shown in Figure 2.

ASPEN results for this model are shown in Table 3.

Table 3: Stream properties of catalytic oxidation subsystem

Stream	Mass flow rate (lb/hr)	Total enthalpy (Btu/hr)	Total entropy (Btu/hr °R)
S1	35.66	- 3291.38	1.17
S2	3.45	- 318.44	0.113
S3	3.45	135.9	0.71
S4	3.45	309.64	0.86
S5	3.45	309.33	0.86
S6	3.45	-145.0	0.39
S7	32.21	-2972.98	1.05
S8	32.21	-2975.56	1.05
S9	35.66	-3120.25	1.49

Q1	Heat duty :	173.7	(Btu/hr)
Q2	Heat duty :	- 0.297	(Btu/hr)
Q3	Heat duty :	- 2.56	(Btu/hr)

The lost work analysis of each unit operation block comprising the catalytic oxidation subsystem is shown in Table 4.

Table 4: Lost work estimation of catalytic oxidation subsystem.

Unit opreation block	Lost Work (Btu/hr)	% of total lost work
Diverter	0	0
Heat Exchanger	67.31	38.2
Heater	79.5	45.1
HTCO	0.297	0.17
LTCO	2.56	1.45
Mixer	26.5	15.04
Total lost work	176.17	

W_{ideal} = 530 (1.49 - 1.17) - (- 3120.25 + 3291.38)

= - 1.53 Btu/hr

This is a nonspontaneous process. Hence

W_S = 1.53 + 176.17

= 177.7 Btu/hr

$\eta_2 = \frac{1.53}{177.7}$

= 0.86%

BOSCH SUBSYSTEM :

The Bosch subsystem was chosen for CO_2 reduction. The design for our model is based on a design proposed by Minemoto et al, [14]. A series of two reactors are used. The first reactor is at a temperature of 1300 [K] while the other reactor is operating at a temperature of 900 [K]. The reactions are given by :

Reactor 1

$$CO_2 + H_2 \leftrightarrow CO + H_2O \quad (12)$$

Reactor 2

$$CO + H_2 \leftrightarrow C + H_2O \quad (13)$$

Since all the CO_2 is eventually converted to C a stoichiometric ratio of H_2 to CO_2 is maintained.

The properties of the streams present in the Bosch subsystem as obtained from our model are shown in Table 5.

Table 5: Stream properties of Bosch subsystem

Stream	mass flow rate (lb/hr)	total enthalpy (Btu/hr)	total entropy (Btu/hr °R)
S1	0.048	-183.79	-6.04×10^{-4}
S2	4.37×10^{-3}	-54.16×10^{-6}	-5.98×10^{-7}
S3	0.398	-677.1	- 0.139
S4	0.398	515.04	0.778
S5 solid	1.3×10^{-2}	4.51	4.27×10^{-3}
S5 vapor	0.385	-130.4	0.436
S6	3.9×10^{-2}	- 268.11	- 0.087
S7 solid	1.3×10^{-2}	-0.08	-1.5×10^{-4}
S7 vapor	0.346	-507.11	-0.177
S8	1.3×10^{-2}	-0.015	-2.87×10^{-5}
S9	0.398	- 677.1	-0.139
Q1	Heat duty:	1192.14	Btu/hr
Q2	Heat duty:	-640.93	Btu/hr
Q3	Heat duty:	-649.41	Btu/hr

Table 6 indicates the amount of lost work in each functional unit comprising the Bosch subsystem.

Table 6: Lost work analysis of unit operation block of Bosch subsystem

Unit operation block	Lost work (Btu/hr)	%lost work
Mixer	6.89	0.55
Reactor 1	486.01	39.04
Reactor 2	461.95	37.11
Condensate Remover	276.13	22.18
Solid carbon remover	13.78	1.11

Total lost work	1244.76	

$$W_{ideal} = 530\,(-2.87\times10^{-5} - 0.087 + 6.21\times10^{-4} + 5.98\times10^{-7} - 1.72\times10^{-5}) - (-286.11 - 0.015 + 178.94 + 54.16\times10^{-6} + 4.85)$$

$$= 38.53 \text{ Btu/hr}$$

Hence this is a spontaneous process.

$$W_s = 38.53 - 1244.76$$
$$= -1206.23$$

This is an example of a highly nonideal process. The actual process is spontaneous. Under simulated working conditions the total irreversibilities within the process is greater than the amount of work generated by the process. Thus the process requires external work to be supplied. Thereby the second law efficiency cannot be meaningfully defined for this subsystem.

STATIC FEED WATER ELECTROLYSIS :

This technique is used for O_2 generation. Our model is based on a design proposed by Fortunato et al [15]. In this method, the water from the water regeneration system is electrolyzed in a water retention matrix to produce H_2 and O_2. The electrolysis chamber is maintained at 30psia. The ASPEN model for the process is shown in Figure 4. The water from the water regeneration unit is pressurized to 30 psia before being fed into the electrolysis chamber. A cooler is used prior to the electrolysis chamber to remove the heat generated due to compression of water. The compressed water is cooled to ambient temperature before being fed into the electrolysis cell. Since there are no tailor made blocks to simulate the reactions occuring at the electrodes in ASPEN, the reaction was simulated using a RSTOIC block.

Table 7: Properties of streams present in the water electrolyis subsystem

Stream	Mass flow rate (lb/hr)	Total enthalpy (Btu/hr)	Total entropy (Btu/hr °R)
S1	9.6×10^{-2}	-654.8	-0.21
S2	9.6×10^{-2}	-654.83	-0.21
S3	9.6×10^{-2}	-654.86	-0.21
S4	9.6×10^{-2}	-0.38	-0.27
S5	1.07×10^{-2}	-0.25	-4.76×10^{-4}
S6	8.52×10^{-2}	-0.13	-2.46×10^{-4}
Q1	Heat duty: - 0.03 Btu/hr		
Q2	Heat duty: 654.55 Btu/hr		

Table 8 presents an analysis of the lost work within each subsystem.

Table 8: Lost work analysis within the water electrolysis subsystem

Unit operation block	Lost work (Btu/hr)	%lost work
Pump	0.427	0.38
Cooler	0.03	0.03
Electrolyzer	96.99	87.08
Gas separator	13.93	12.51
Total lost work	111.38	

$$W_{ideal} = 530\,(-4.76\times10^{-4} - 2.46\times10^{-4} + 0.21) - (-0.13 - 0.25 + 654.8)$$

$$= -543.5 \text{ Btu/hr}$$

Thus this is an example of a nonspontaneous process.

$$W_S = -654.88 \text{ Btu/hr}$$

$$\eta_2 = \frac{543.5}{654.88}$$

$$= 82.99\%$$

HUMIDITY CONDENSATE SEPARATOR :

In order to maintain the cabin humidity at a desired level, the humidified exit air from the trace removal subsystem is cooled to a temperature such that the amount of moisture in the air leaving the condenser separator is equal to the amount of moisture to be supplied to the cabin. The amount of moisture present in the air which is supplied to the cabin is calculated in a FORTRAN block by taking into account the desired humidity level to be maintained in the cabin and the moisture level of the expired air from the crew. The condensate is removed and treated to obtain water of potable quality. For the ASPEN model the condenser separator is modeled as a single unit using a SEP block.The temperature of the condenser is set in a user incorporated FORTRAN subroutine which takes into account the humidity levels of the incoming and outgoing streams.

Table 9: Properties of streams present in the humidity condensate separator

Streem	Mass flow rate (lb/hr)	Total enthalpy (Btu/hr)	Total entropy (Btu/hr °R)
S1	35.66	- 3120.22	1.49
S2	7.18 x 10-2	- 489.58	- 0.154
S 3	35.59	- 2783.35	1.35
Q1	Heat duty:	- 152.71 Btu/hr	

Since the heat of condensation is not being used to do any useful work, hence

$$\text{Lost work} = 530\,(1.35 + 0.154 - 1.49) + 152.71$$

$$= 160.13 \text{ Btu/hr}$$

$$W_{ideal} = 530(1.35 + 0.154 - 1.49) - (-489.58 - 2783.35 + 3120.22)$$

= 160.13 Btu/hr

This is a spontaneous process.

Ws = 0

Thus η_2 = 0

This is valid since we had assumed that the heat of condensation is not used for doing useful work, thereby the amount of work which can be obtained from the process is zero.

SABATIER REACTOR :

The Sabatier reactor is used for CO_2 reduction. The reaction occurs at 350 to 980°F in the presence of ruthenium on alumina catalyst. The reaction mechanism is shown in equation (14)

$$CO_2 + 4H_2 \leftrightarrow CH_4 + 2H_2O + 1790 \text{ btu/lb} \quad (14)$$

Our design for the Sabatier reactor is based on a model proposed by Spina and Lee [16]. A stoichiometric reactant mixture of CO_2 and H_2 is fed into the reactor. The reaction efficiency being higher than 98% a single pass through the reactor is used. The methane and water vapor formed along with the excess reactants are cooled in the condenser where the water is condensed and the remaining gases is sent to the trace removal subsystem. For the ASPEN model the reactor was modelled using a RSTOIC as shown in Figure 6.

Table 10 : Properties of streams present in the Sabatier subsystem.

Stream	Mass flow rate (lb/hr)	Total enthalpy (Btu/hr)	Total entropy (Btu/hr° R)
S1	0.43	-1665.05	5.78×10^{-3}
S2	1.74	-40.87	-0.08
S3	1.26×10^{-3}	-4.84	1.68×10^{-5}
S4	2.17	155.1.	3.34
S5	1.82	-384.23	0.15
S6	0.35	-2377.72	-0.76
Q1	Heat duty = 1866.14 Btu/hr		
Q2	Heat duty = -2917.24 Btu/hr		

Table 11 presents an analysis of lost work within each subsystem.

Table 11 : Lost work analysis in the Sabatier subsystem.

Unit operation Block	Lost work (Btu/hr)	% lost work
Reactor	1807.94	68.6
Condenser	826.92	31.4
	2634.86	

W_{ideal} = 530(0.15 - 0.76 - 5.78×10^{-3} + 0.077 -1.68 ×10-5) - (-2377.72 -384.23 + 1665.05 + 40.87 + 4.84)
= 768.81 Btu/hr

Hence this is a spontaneous process.

W_S = 768.81 - 2634.86
= - 1866.05 Btu/hr

It is thus observed that like the Bosch the Sabatier too is an example of a highly non ideal process from the entropy viewpoint. The second law effciency cannot be meaningfully defined in this case just as in Bosch subsystem. Comparing the two ,Bosch and the Sabatier it is observed that the Bosch is more advantageous compared to the Sabatier since the amount of work required is less for the Bosch.

CONCLUSIONS :

As shown in Tables 2, 4 and 6 lost work analysis provides a means of identifying areas within a subsystem where work is lost due to irreversibilities. The magnitude of second law efficiency of some subsystems like the catalytic oxidation process, the Bosch subsystem or the sabatier subsystem reveal that these subsystems merit considerable attention to redesign their functional units from an entropy minimization viewpoint.

For example, our study shows that percentage of lost work in the reactors used for CO_2 reduction is between 35 to 39 %. It is hoped that this insight will encourage designers to redefine the operating conditions so as to optimize between yield of desired product and lost work.

It is justified to mention here that due to unavailibility of detailed hardware information it was not feasible to obtain a detailed estimate of energy required for a particular subsystem. However this is not a violation of our primary objective which is to demonstrate the potential of the lost work analysis in redesigning the existing ECLSS technologies.

The overall conclusion to be drawn from this paper is that there exists a potential for higher efficiency in the currently used ECLSS technologies which warrants evaluation of the present operating conditions.

REFERENCES :

[1] Brandhorst,Jr.,H.,W.," Energy Requirement for the Space Frontier," Paper No. 912064, Twenty first Intersociety Conference on Environmental Systems, San Francisco, 1991.

[2] Cook,E., Sci.Am, 225, 83, 1971.

[3] Reistad, G.,M., Trans ASME J., Engng Power, 97, 429, 1975.

[4] Keenan, J.,H., Mech Engng, 54, 195, 1932.

[5] Guoy, G., J. physique, 8, 501, 1889.

[6] Stodola, A., Zeitschrift, VDI, 32, 1086, 1898.

[7] Herbert, W., H., and Stephen, C.,H.," Second Law Analysis : An Alternative Indicator of System Efficiency", Energy, 5, 865 - 874, 1980.

[8] Ahern, J.E., " Applicatins of the Second Law of Thermodynamics to Cryogenics - A Review", Energy, 5, 891 - 898, 1980.

[9] Nevers,N.D., Seader, J.D., " Lost Work. A Measure of Thermodynamic Efficiency", Energy, 5, 757 - 769, 1980.

[10] Smith, J.,M., and Van Ness, H.,C., Introduction to Chemical Engineering Thermodynamics, Mc Graw- Hill Book Company, 4th edition, 548 - 564. 1987.

[11] Rohatgi,N., et al.," Human Life Supporrt During Interplanetary Travel and Domicile, Part - 2 : Generic Modular Flow Schematic Modeling", Paper No. 911332, Twentyfirst Intersociety Conference on Environmental Systems, San Francisco, 1991.

[12] Takahashi,Y., Ohya,H.," Wet-Oxidation Waste Management System for CELSS", Paper No. 851398, Fifteenth Intersociety Conference on Environmental Systems, Portland, 1985.

[13] Ammann, K.," Development of the Catalytic Oxidizer Technology for the European Spcae Program", Paper No. 891539, Nineteenth Intersociety Conference on Environmental Systems, San Diego, 1989.

[14] Minemoto, M., et al., " Study of Air Revitalization System for Space Station", Paper No. 891576, Nineteenth Intersociety Conference on Environmental Systems, San Diego, 1989.

[15] Fortunato, F., A., et al.," Static Feed Water Electrolysis System for Space Station Oxygen and Hydrogen Generation", Paper No. 880994, Eighteenth Intersociety Conference on Environmental Systems, San Francisco, 1988.

[16] Spina,L., and Lee,M.,C., " Comparison of CO2 Reduction Process- Bosch and Sabatier", Paper No 851343, Fifteenth Intersociety Conference on Environmental Systems, Portland, 1985.

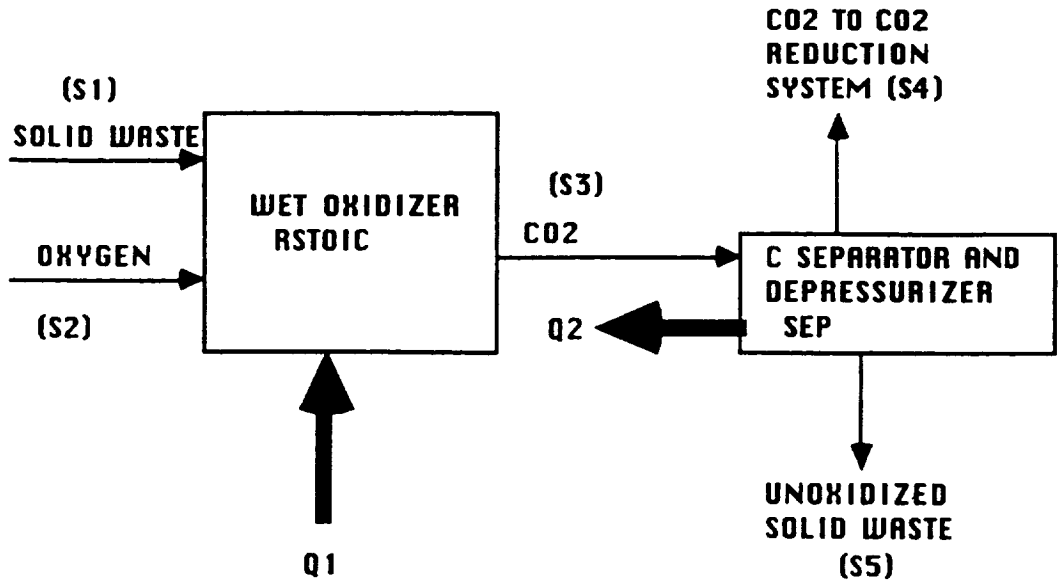

Figure 1: Schematic of solid waste wet oxidation subsystem.

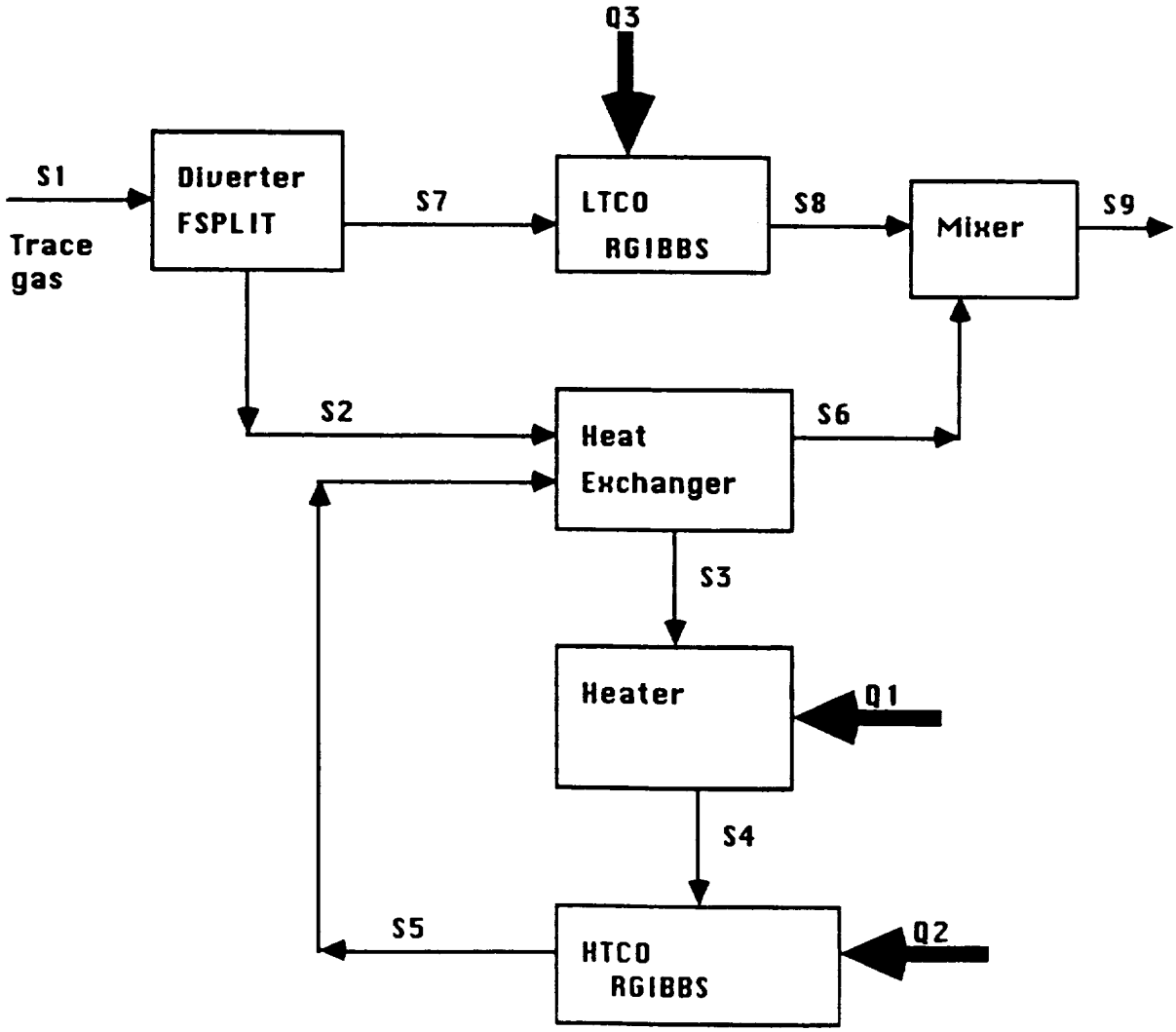

Figure 2: Schematic of catalytic oxidation subsystem

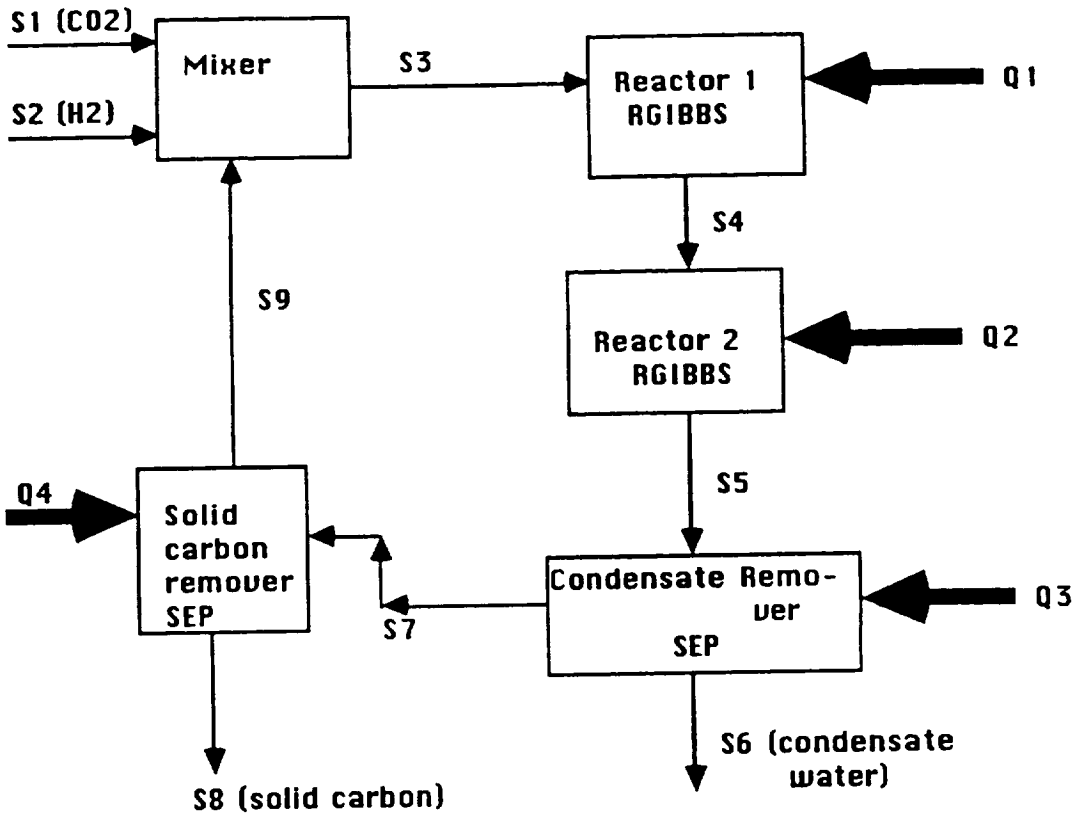

Figure 3: Schematic of Bosch subsystem

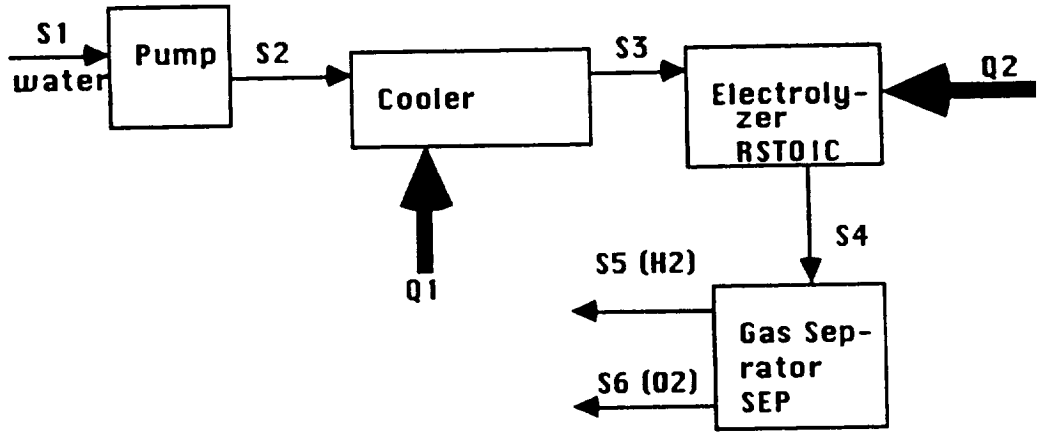

Figure 4: Schematic of water electrolysis subsystem

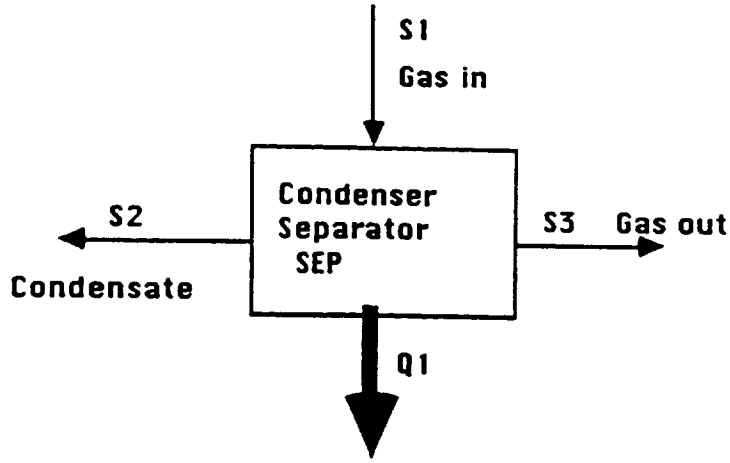

Figure 5: Schematic of humidity condensate separator

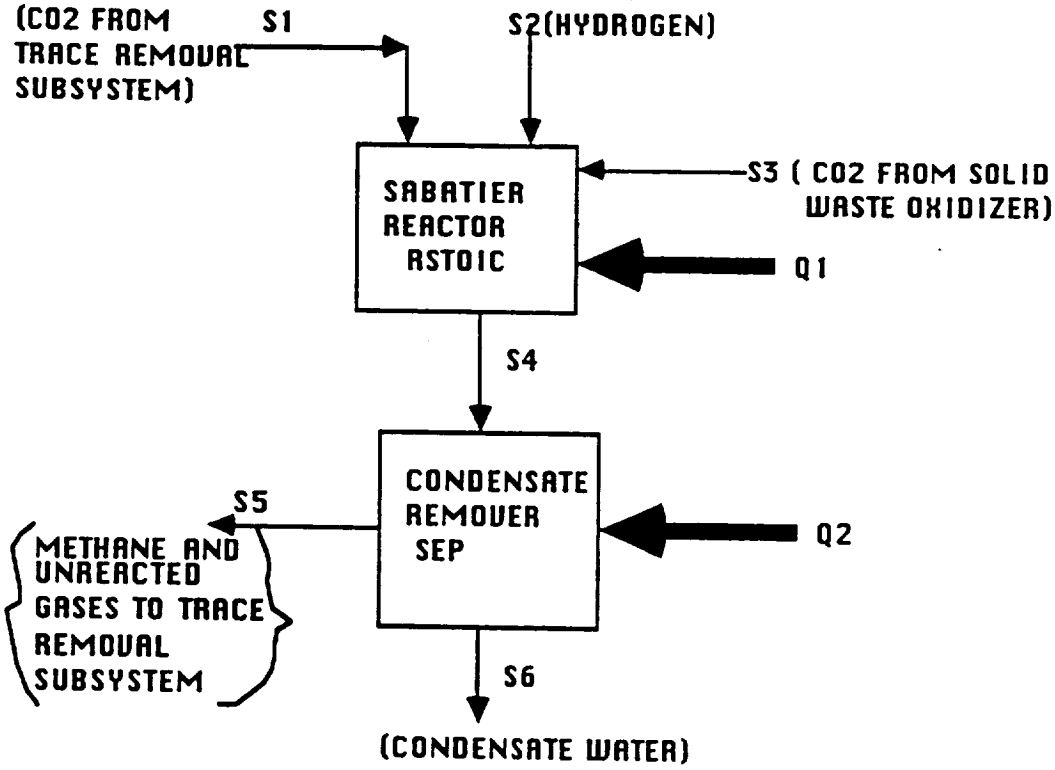

Figure 6: Schematic of Sabatier subsystem